OXFORD JOURNAL
OF STUDENT
SCHOLARSHIP

Unravelling Cytotoxicity Profile Differences in Structurally Similar Metal-Organic Frameworks

Tarika T. Chari
charit@asbindia.org

ABSTRACT

Metal-organic frameworks (MOFs) have emerged as highly tunable nanomaterials with significant promise for biomedical applications, but their cytotoxicity profiles vary considerably across structural variants. This review synthesises comparative studies of structurally similar MOFs to establish structure-toxicity relationships, where such MOFs variants are defined as frameworks differing only by one key parameter, such as metal node, linker chemistry, surface functionalisation, or particle size. Evidence consistently shows that the choice of metal node is the primary determinant of toxicity. Frameworks based on redox-inert metals, including Zr, Al, and Cr, exhibit high stability and favourable biocompatibility, whereas MOFs incorporating Cu or Mn nodes often induce cytotoxicity through redox cycling and reactive oxygen species (ROS) generation. Linker chemistry further modulates toxicity by influencing polarity and hydrolytic stability. For example, fumarate and 1H-imidazole-2-carbaldehyde (HICA) linkers promote rapid degradation and oxidative stress, while aromatic linkers such as trimesic acid, terephthalic acid, and biphenyldicarboxylate provide enhanced stability and lower toxicity. Surface functionalisation introduces cell-type-specific effects: amine or nitro groups can enhance uptake and ROS generation, while hydrophobic modifications alter aggregation behaviour and circulation time. Particle size also plays a dual role, with nanoscale particles increasing dissolution-driven toxicity and larger micron-sized particles exerting mechanical stress on cells. Collectively, these findings highlight how subtle structural differences critically shape the biological behaviour of MOFs. By mapping these structure–toxicity relationships, this review provides mechanistic insights and design principles to guide the safe and effective development of MOFs for biomedical use.

INTRODUCTION

Metal-organic frameworks (MOFs) are a promising group of porous materials first predicted in 1990, and then termed in 1995, with early work by Yaghi and colleagues synthesising the first MOF in 1990[1]. This was the establishment of modular creation and extremely tunable MOF structures. These materials have two key components that make up their structure: inorganic metal ions or clusters that form metal nodes, and organic linkers that connect these nodes together, which together create extended three-dimensional

frameworks with high surface areas and porosity. Over the last three decades, MOFs have become a larger focus due to their potential for a wide variety of applications, with thousands synthesised and investigated for uses such as gas storage and catalysis to separation technologies. Among these applications, the biomedical field has been researching MOFs for their potential in biosensing, imaging, photodynamic therapy, and drug delivery[2,3,4].

The history and evolution of MOFs can be tracked through a series of milestones that eventually set up the framework needed for biomedical usage. Over the past three decades, several thousands of MOFs have been synthesised and according to the Cambridge Crystallographic Data Centre, the Cambridge Structural Database contains over 100,000 MOFs[60]. There is now increasingly greater attention from scientists towards their suitability for biomedical applications due to their stability and tunability. For example, HKUST-1 is a copper-based MOF developed in 1999, and it was one of the earliest frameworks to receive widespread attention for its high porosity[5]. The MIL-series (Materials of Institute Lavoisier), particularly MIL-100 and MIL-101, was introduced next and uses iron(III)-based frameworks with large cages that can host guest molecules[6]. Another milestone was the creation of zirconium-based UiO-66, which has strong chemical and thermal stability, and created a benchmark for biocompatible MOFs[7]. Among the earliest MOFs to be explored for biomedical use was ZIF-8 (zeolitic imidazolate framework-8), a zinc-based MOF constructed from 2-methylimidazolate linkers. ZIF-8 attracted attention because of its unique pH-responsive degradation profile-remaining stable at physiological pH but rapidly disassembling under acidic conditions, such as those encountered in endosomes or lysosomes[8]. This property made it a particularly attractive candidate for drug delivery and controlled release applications. Recent advances have resulted in porphyrinic MOFs (PCNs) with integrated photoactive properties, as well as nanoscale MOFs (nMOFs) designed specifically for biomedical applications[9]. These structural innovations and milestones have expanded the relevance of MOFs in the biomedical sphere, and have laid the foundation for their use in drug delivery and other biomedical applications.

STRUCTURAL OVERVIEW AND CLASSIFICATION OF MOFs

MOFs are produced by the formation of chemical bonds between organic ligands as linkers and metal ions as nodes, leading to formation of periodic network crystalline structures with high porosities and

large surface areas[25, 26, 46]. They have a flexible design, which offers vast structural variety and broad capabilities to form objects with customised properties[25].

MOFs are made by bonding a metal ion with organic linkers by coordination (Figure 1) and comprise both organic and inorganic components[9]. The organic components (linkers) include a conjugate base of a carboxylic acid or anions, such as organophosphorus compounds, salts of sulfonic acid, and heterocyclic compounds as shown in Figures 2 & 3. The inorganic elements are metal ions or clusters called secondary building units (SBUs). Its geometry is determined by the coordination number, coordination geometry of the metal ions, and the nature of the functional groups[9]. A variety of SBU geometries with different number of points of extension such as octahedron (six points), trigonal prism (six points), square paddle‐wheel (four points), and triangle (three points) have been observed in MOF structures (Figure 4)[9]. In principle, a bridging ligand (ditopic, tritopic, tetratopic, or multitopic linkers) reacts with a metal ion with more than one vacant or labile site. The final framework topology of MOF is governed by both SBU connectors and organic ligand linkers[9].

The structural classification of MOFs provides insights into the way we think about organizing and characterizing the ever-expanding library of the synthesised MOFs. Several approaches have been proposed to classify the structural characteristics of MOFs, but there is no single and comprehensive classification of MOFs given wide range of MOF varieties and complexity of interconnected structures. Some common structural classifications that provide insights into the arrangement of metal nodes, organic linkers and structural spaces are as follows[10]:

Topological Classification: One of the most widely employed structural classifications of MOFs is based on their network topology. This classification considers the connectivity and arrangement of metal nodes and organic linkers within the framework. Topology determines the overall architecture and shape of the MOF structure and is often represented using a graph-based representation known as a net or a coordination network. Examples of MOF topologies include MIL-53, with a diamond-shaped network and UiO-66, with a Zr-based octahedral node and a linear linker[10,46].

Dimensionality-based Classification: MOFs can be classified based on dimensionality, which refers to the number of spatial dimensions in which the framework extends. The three common dimensionalities observed in MOFs are zero-dimensional (0D), one-dimensional (1D), and three-dimensional (3D)[10]. Zero-dimensional MOFs represent discrete clusters or isolated metal sites, while one-dimensional MOFs exhibit chain-like structures. Three-dimensional MOFs form extended networks with porous

architectures. This classification provides insights into the connectivity and arrangement of metal nodes and linkers within the MOF framework[10].

Cage-Based Classification: Some MOFs possess shaped spaces or cages within their structures. These cage-based MOFs are classified based on the shape, size, and connectivity of these spaces. For example, cubic or octahedral cages are commonly found in zeolitic imidazolate frameworks (ZIFs), while hexagonal prismatic and concave coordination cages are characteristic of metal-organic polyhedral (MOPs) or coordination polymers (CPs)[10].

Functional Group-based Classification: Another approach to classifying MOFs is based on the types of functional groups present in the organic linkers[10]. Organic linkers can incorporate various functional groups, such as carboxylate, pyrazolate, imidazolate, phosphonate, amine, or hydroxyl groups. The presence of different functional groups gives specific chemical properties to the MOFs, affecting their reactivity, selectivity, and adsorption capabilities[10]. This classification provides insights into the chemical diversity and potential applications of MOFs based on the functional groups present in their structures.

It is important to note that these classifications are not mutually exclusive, and multiple criteria can be combined to provide a comprehensive understanding of MOF structures.

SURFACE FUNCTIONALISATION

Surface functionalisation refers to the deliberate modification of the external surface of MOF particles with chemical groups, polymers, or biomolecules, while leaving the underlying framework structure intact. Unlike changing the internal pore chemistry alone, surface functionalisation directly controls how MOFs interact with their surrounding biological environment;for example, by influencing colloidal stability, protein corona formation, immune recognition, or cellular uptake[24]. It is therefore considered a powerful strategy for tuning the chemical, physical, and biological properties of MOFs without altering their intrinsic topology. Functionalisation can be achieved through pre-synthetic approaches, where functional groups are incorporated into the organic linker or metal node during synthesis, or through post-synthetic modification (PSM), which introduces new moieties onto preformed frameworks[9]. Pre-synthetic strategies allow predictable control over pore chemistry and framework polarity, enabling systematic design of hydrophilic, hydrophobic, or charged environments. In contrast, PSM provides greater modularity, allowing the attachment of biomolecules, targeting ligands, fluorescent tags, or

catalytic groups while preserving crystallinity. For example, PEGylation or polymeric surface coatings can improve colloidal stability and reduce immunogenicity. For instance, non-functionalised MIL-100(Fe) nanoparticles agglomerate after a short period of time under physiological conditions, but when cyclodextrin, heparin, or crosslinked polyethylene glycol (PEG) are anchored onto their external surface their colloidal and chemical robustness is significantly enhanced[11,12,13]. A study by Giménez-Marqués et al.[11] focused on improving the biomedical applicability of MOFs by modifying their outer surface in a safe and effective way. The authors used a novel "GraftFast" method, a green and simple grafting strategy, to attach biopolymers such as polyethylene glycol (PEG) and hyaluronic acid to the surface of nano-sized MIL-100(Fe) particles. This method avoided the drawbacks of conventional surface modification techniques, which can sometimes cause toxicity or lack specificity. The PEGylated MIL-100(Fe) nanoparticles showed high stability in different biological fluids while preserving their internal porosity, meaning they could still adsorb and carry bioactive molecules like anticancer drugs. Using advanced X-ray spectroscopy, the researchers explored the nature of the interaction between PEG and the MOF surface, confirming the robustness of the coating. Finally, drug-loading experiments with radio-labeled gemcitabine monophosphate demonstrated that PEG coating not only enabled efficient drug delivery but also reduced macrophage uptake, giving the particles a “stealth” effect that helps them evade immune clearance. Similarly, Agostoni et al.[12] used cyclodextrin molecules modified with strong iron-binding groups (phosphates), which could anchor firmly to iron-based MOF surfaces simply by incubating in water for a few minutes. This coating process preserved the nanoMOF’s porosity, crystallinity, and drug adsorption/release properties, ensuring that the functional advantages of MOFs were not compromised. Moreover, the cyclodextrin coating could be further engineered by (i) With targeting ligands, to enhance receptor-specific uptake, and (ii) With PEG chains, to reduce immune clearance. Bellido et al.[13] coated MIL-100(Fe) nanoMOFs with heparin, a natural biopolymer known for prolonging circulation times in vivo. The heparin coating preserved the structural integrity and porosity of the MOFs while improving colloidal stability under physiological conditions. Importantly, the coating did not impair their drug encapsulation and release capacities. Biological evaluations revealed that heparin-functionalised MIL-100(Fe) nanoparticles had reduced immune recognition, no activation of the complement system, and lower production of reactive oxygen species (ROS), while also minimizing inflammatory cytokine release. These findings showed that the heparin coating improved biocompatibility and reduced immunotoxicity, highlighting surface functionalisation as a critical step in enhancing the biomedical potential of nanoMOFs.

Besides the improvement of colloidal and chemical stability, surface modifications have also been reported as effective tool for the selective cytotoxicity and targeted delivery of MOF nanoparticles, such as Zr-Fumarate,[14] and UiO-66(Zr)[15]. Abánades Lázaro[14] showed that PEGylation of Zr-fum improved its cellular uptake, particularly through caveolae-mediated endocytosis, and enhanced its selective cytotoxicity against cancer cells (HeLa and MCF-7) while sparing healthy kidney cells, macrophages, and lymphocytes. When compared with UiO-66, Zr-fum showed greater efficiency in delivering calcein (a drug mimic) into HeLa cells and stronger anticancer effects when loaded with DCA and PEGylated. Immunological assessments revealed that PEGylated Zr-fum produced less reactive oxygen species (ROS) than UiO-66, likely due to the biocompatible fumarate linker, and it did not activate the complement cascade (C3 and C4), suggesting reduced immune recognition and lower risk of phagocytic clearance. Another study by Abánades Lázaro[15], focused on improving the stability and drug delivery performance of the zirconium-based MOF UiO-66 through a novel surface-modification approach called "click modulation." In this method, UiO-66 nanoparticles (~200 nm) were synthesised with surface-functionalised modulators, loaded with drugs, and then covalently PEGylated using mild bioconjugation reactions. The PEG chains played a dual role, (i) At physiological pH (7.4), they improved the MOF's stability against degradation by phosphates (which would normally break down Zr-based frameworks) and reduced the undesirable "burst release" of drugs by shielding surface interactions. (ii) At acidic pH (5.5), mimicking lysosomal/tumor environments, the PEGylated MOFs achieved stimuli-responsive drug release, making them more effective in targeted therapies. Importantly, surface chemistry influenced the pathway of cellular uptake. PEGylated UiO-66 particles were more likely to enter cells via caveolae-mediated endocytosis rather than the usual lysosomal pathway. This is significant because avoiding lysosomal degradation allows more drug to reach the cytosol intact. When loaded with dichloroacetic acid (DCA), the PEGylated UiO-66 showed enhanced cytotoxicity, underscoring its potential as an efficient drug delivery system. The broader implication is that click modulation provides a versatile and biofriendly method to tailor MOF surfaces with polymers like PEG, which can improve stability, control release profiles, and optimise cellular trafficking for drug delivery.

Another interesting aspect of surface functionalisation is their impact on drug release kinetics. Especially for a high efficiency drug delivery in cancer therapy; the coating of different MOF nanoparticles, such as MFU-4l(Zn), UiO-66(Zr) or ZIF-8(Zn) with PEG turned out to be very powerful to gain a better control over drug release kinetics.[15,16,17]. Ettlinger et al.[16], explored how arsenic trioxide (ATO), a drug that is both a potent anticancer agent and a well-known poison, could be made safer and more effective using functionalised MOFs as nanocarriers. While ATO works well in leukemia, its high toxicity has prevented

its use in treating solid tumors, despite evidence that it could be highly effective against aggressive cancers such as atypical teratoid rhabdoid tumors (ATRTs) which is a rare pediatric brain tumor. To address this, the researchers used a zinc-based MOF called MFU-4l, built from Zn(II) ions and special triazole–dibenzo ligands, to encapsulate ATO in the form of dihydrogen arsenite anions ($H_2AsO_3^-$). This was achieved through a postsynthetic ligand exchange process, allowing the toxic drug to be stably incorporated into the MOF nanoparticle framework. The resulting drug release studies showed that ATO could be released in a pH-responsive manner, meaning more drug was released under acidic conditions (like those in tumor microenvironments), while stability was maintained under physiological conditions. Finally, cytotoxicity experiments on ATRT cell lines demonstrated that the MOF-encapsulated ATO retained its anticancer effect but with the potential for reduced systemic toxicity, since controlled release lowers the risk of overdosing healthy tissues. Tests on non-tumor control cell lines suggested better selectivity compared to free ATO. Overall, the study demonstrated that surface functionalised MFU-4l MOFs could act as a safe and effective nanocarrier for arsenic trioxide, offering a way to repurpose this old but powerful drug for the treatment of solid tumors like ATRT, where traditional formulations are too toxic to use. In a follow up study, Ettlinger et al.[17] build on their earlier work with arsenic trioxide as an anticancer drug, but here they focus on using ZIF-8, a zeolitic imidazolate framework, as the carrier system. They loaded As(III) species into ZIF-8 nanoparticles with PEG surface coating and observed that at neutral pH (7.4, like blood), only minimal arsenic was released, meaning the carrier remains stable in healthy tissue. At acidic pH (tumor or lysosome-like conditions), the drug was fully released, showing ZIF-8's pH-triggered delivery works effectively. *In vitro* cytotoxicity tests showed the As(III)-loaded ZIF-8 nanoparticles were much more toxic to cancer cells than to fibroblasts (healthy cells). This suggests selective activity against tumors while sparing normal tissue. Together, these approaches establish functionalisation as a central design tool for biomedical MOFs.

MOFs can also be conjugated with ligands such as transferrin, folic acid, peptides, or antibodies, enabling receptor-mediated uptake by specific cell types and thereby improving therapeutic precision[18,19]. Such approaches not only enhance drug delivery efficiency but also reduce off-target toxicity, since functionalised MOFs can exploit natural receptor-ligand interactions to selectively accumulate in diseased tissues. This strategy is particularly valuable in cancer therapy, where overexpressed receptors provide molecular "entry points" for functionalised nanocarriers. A recent study by Serag et al.[18] exemplifies this approach through the development of a folic acid-conjugated MIL-101(Fe) nanocarrier loaded with the anticancer agent 1,8-acridinediones (DO8). The folic acid modification enabled selective targeting of HepG-2 liver cancer cells, which overexpress folate receptors, while maintaining high colloidal stability

under physiological conditions. Importantly, the system demonstrated pH-responsive DO8 release in acidic environments mimicking the tumor microenvironment, ensuring controlled intracellular delivery. Upon light activation, the nanocomposite generated high levels of ROS, enhancing photodynamic therapy efficacy in combination with chemotherapy. The dual-therapy system showed markedly lower IC_{50} values under light conditions compared to dark, with necrosis driven by ROS-induced membrane rupture identified as the primary mechanism of cell death. This study underscores the dual benefits of surface functionalisation: receptor-mediated specificity and synergistic therapeutic action, highlighting the potential of targeted, multifunctional MOFs in precision oncology. Another example of selective targeting functionalisation comes from the work of Wu et al.[19], who developed a biomimetic ZIF-8 platform for brain-targeted therapy. In this study, ZIF-8 nanoparticles were coated with RVG15-PEG conjugates, leveraging the rabies virus glycoprotein-derived RVG15 peptide to achieve efficient penetration across the blood–brain barrier (BBB). The resulting RVG15-PEG@DTX@ZIF-8 particles not only displayed high stability and drug-loading capacity but also demonstrated selective accumulation in glioblastoma tissue following systemic administration. The RVG15 peptide mediated rapid nanoparticle entry into the brain, while PEG improved colloidal stability and circulation time, together ensuring effective biodistribution. In vivo, this functionalisation strategy enabled docetaxel-loaded ZIF-8 nanoparticles to inhibit tumor growth, reduce metastasis, and significantly improve survival in glioblastoma-bearing mice. This work highlights how surface functionalisation with targeting peptides can exploit natural receptor-mediated pathways, allowing MOFs to overcome the restrictive BBB and deliver chemotherapeutic payloads directly to the brain. Such ligand-mediated strategies highlight how functionalisation enables MOFs to operate in highly selective and biologically complex environments.

Beyond synthetic flexibility, functionalisation importantly shapes how MOFs interact with biological systems. Surface polarity and charge influence protein corona formation, a dynamic process in which plasma proteins adsorb onto the nanoparticle surface. This corona determines biodistribution, immune recognition, and cellular uptake[20]. Adsorption of protein can negatively affect biological processes, disturb regulatory mechanisms, and also trigger toxic effects of nanoparticles, for instance by enhancing their cellular uptake or by inducing strong complement activation. Cedevervall et al.[20] showed a strong dependence of protein adsorption on nanoparticle surface characteristics in their study comparing different copolymers of N-Isopropylacrylamide (NIPAM) and N-tert-butylacrylamide (BAM). The residence time of albumin was shorter on the more hydrophobic nanoparticles compared with the more hydrophilic nanoparticles. Hydrophilic or charged groups, such as $-NH_2$, promote hydrogen bonding and protein adsorption, which may accelerate clearance by macrophages through opsonization. Conversely,

hydrophobic moieties such as -CH_3 reduce nonspecific interactions and enhance circulation stability. González-García et al.[21] demonstrated that surface functionalisation plays a decisive role in how nanomaterials interact with biological systems, particularly through protein corona formation and immune responses. Using a simple plasma polymerization method, silica nanoparticles were coated with different chemical groups, namely carboxylic acid, oxazoline, amine, and hydrocarbons, without altering their core structure. When exposed to blood serum or plasma, all nanoparticles formed protein coronas enriched in smaller molecular weight proteins, likely due to their curved surfaces. However, the composition of the coronas varied significantly with surface chemistry, which in turn shaped immune responses. Hydrocarbon-coated nanoparticles formed albumin-rich coronas that stimulated macrophages to release pro-inflammatory cytokines such as IL-6 and TNF-α. Similarly, carboxylic acid coatings increased inflammatory cytokine production but were associated with coronas enriched in complement proteins and reduced lipoproteins. In contrast, amine-rich coatings promoted an anti-inflammatory profile, enhancing arginase expression in macrophages. These findings highlight how engineering nanoparticle surface chemistry can be used to tailor physiological responses, by promoting immune activation for applications such as vaccines, or dampening immune recognition for safer drug delivery systems.

Functional groups can also influence the intracellular fate of MOFs, particularly during endocytosis and lysosomal processing. Ruenraroengsak et al.[22] in their study show that amine-modified polystyrene nanoparticles (50–100 nm) caused severe membrane disruption in alveolar epithelial cells, producing visible holes, cell detachment, and apoptosis via caspase activation, alongside an inflammatory response marked by elevated CXCL8 (IL-8). In contrast, unmodified or carboxyl-modified particles of similar size, as well as larger 100 nm particles, showed minimal cytotoxicity. These observations highlight the heightened reactivity of positively charged amine groups, which interact strongly with the negatively charged phospholipid membranes, leading to destabilization and subsequent cell death. In contrast, the work of Li et al.[23] highlights how biomimetic mineralization with ZIF-8 can be used to control nanoparticle–biomolecule interactions, which is directly relevant to lysosomal processing and intracellular stability of MOFs. By coating viral nanoparticles such as tobacco mosaic virus (TMV) with ZIF-8, the study demonstrated how mineralised shells can protect sensitive biological cargos from enzymatic degradation. Importantly, the results show that the morphology of TMV@ZIF-8 composites depends strongly on crystallization parameters and the strength of virus–Zn^{2+} interactions. These findings parallel the intracellular context, where MOFs undergo endocytosis and encounter acidic lysosomes: frameworks like ZIF-8 degrade under acidic conditions, releasing their encapsulated biomolecules into the cytosol. The Li study[23] therefore provides a model system for understanding how nanoscale

MOF–biomacromolecule composites can be tuned through functionalisation to survive extracellular environments yet respond to intracellular cues such as lysosomal acidification.

Taken together, functionalisation transforms MOFs into multifunctional biomedical platforms. While the underlying crystalline topology defines stability and porosity, surface modifications dictate how MOFs are perceived by biological systems, how long they circulate, where they distribute, and how they interact at the cellular and subcellular levels. By balancing synthetic design with biological performance, functionalisation ensures that MOFs are not only structurally versatile but also biologically adaptive-positioning them as powerful candidates for drug delivery, imaging, catalysis, and beyond.

MOF INTERACTIONS WITH BIOLOGICAL ENVIRONMENTS

Once introduced into the body, MOFs encounter a series of physiological barriers and dynamic chemical conditions that determine their stability, distribution, and bioactivity. Factors such as pH, redox state, enzymatic activity, and protein adsorption can dramatically alter particle surface properties, degradation kinetics, and cellular responses[10,30]. Understanding these environment-specific behaviours is critical for predicting MOF performance in biomedical applications.

In the case of intravenous administration, once administrated, the first key environment a MOF encounters is the bloodstream, where protein adsorption, aggregation, and ion exchange can all influence both biodistribution and clearance[24]. Upon entering the bloodstream, MOFs are rapidly coated with a protein corona of plasma proteins, which changes their surface properties and influences how the body reacts to them[10,30]. Hydrophobic or positively charged MOFs often attract opsonins which tag foreign particles, promoting clearance by macrophages, whereas hydrophilic coatings such as polyethylene glycol (PEG) can extend circulation time[11]. Protein corona formation has also been shown to significantly modulate the cytotoxicity of Cu-based MOFs, highlighting the protective role of this dynamic layer[25]. A study by Jafari et al.[25] highlights how both the structural properties of copper-based MOFs and their interactions with biological components influence their biomedical potential. The researchers showed that for Cu-MOF (MOF-1) when plasma proteins formed a corona on MOF-1, the overall cytotoxicity against cancer cell lines was reduced. The protective effect was attributed to the corona masking the MOF's structural and chemical features, preventing direct contact between the nanoparticle surface and the cells. However, the MOFs still displayed concentration-dependent toxicity in the absence of plasma proteins,

with higher concentrations increasing cell death. These results suggest that while uncoated MOF-1 structures can display inherent cytotoxicity, protein corona formation substantially mitigates this effect and may enhance their safety profile. Furthermore, as discussed earlier, surface functionalisation can further fine tune the interaction of the MOF with protein corona[20,21].

The digestive system is also a common environment encountered by MOFs, where pH gradients and enzymatic conditions can drive rapid degradation of MOF frameworks. Orally administered MOFs must endure the acidic conditions of the gastrointestinal (GI) tract where the digestive enzymes can degrade susceptible MOFs such as ZIF-8, triggering early release of ions or cargo and can cause toxicity[10,30]. By contrast, Zr-based MOFs, such as UiO-66 derivatives, exhibit superior acid resistance due to strong Zr-O bonds. This also highlights the importance of encapsulation strategies, such as sodium alginate hydrogels embedding MOFs, which can then enhance stability in gastric fluid and enable colon-targeted delivery[26]. A study by Gao et al.[26] uses MOF encapsulation to address a key problem in treating ulcerative colitis (UC), an inflammatory bowel disease that can progress to colorectal cancer. Conventional oral drugs and antibody therapies face challenges such as poor bioavailability, systemic toxicity, or limited effectiveness in maintaining long-term remission. Small interfering RNA (siRNA) offers a more targeted and potentially safer approach by silencing specific inflammatory genes, but it is highly unstable in the gastrointestinal (GI) tract and typically gets degraded before reaching the colon. To overcome this, the researchers designed a hybrid delivery system where siRNA targeting TNF-α (a key inflammatory cytokine) was loaded into a MOF carrier, and this MOF-siRNA complex was further encapsulated in sodium alginate (SA) hydrogel particles (SA@MOF-siRNA$^{TNF\alpha}$). This design gave a double layer of protection: the alginate shell shielded the MOF and siRNA cargo from acidic gastric fluid and digestive enzymes, while the MOF itself stabilised the siRNA and improved cellular uptake. The results showed that this system survived passage through the stomach and small intestine, specifically accumulated in the colon, and was preferentially taken up by inflammatory macrophages in the diseased tissue. In mouse models of colitis, treatment with SA@MOF-siRNA$^{TNF\alpha}$ reduced typical UC symptoms such as weight loss, bloody stools, and diarrhoea. Mice also showed less tissue damage and inflammation, indicating effective suppression of TNF-α signalling. The study demonstrated that combining MOF nanocarriers with hydrogel encapsulation provides a promising oral delivery strategy for siRNA therapies in UC. This hybrid system not only protects siRNA in the GI tract but also improves colon-specific delivery and therapeutic efficacy, highlighting a path toward safer and more effective treatments for inflammatory bowel diseases.

Another key environment is the blood-brain barrier (BBB), which presents a significant obstacle for nanocarriers, but MOFs can be engineered for receptor-mediated transport to help them cross this barrier and deliver drugs directly to the brain. Surface functionalisation with transferrin or rabies virus glycoprotein (RVG) peptides have shown to enable MOFs to cross the BBB and deliver therapeutics to the central nervous system[19,27]. For example, Chen et al.[27] used transferrin surface functionalisation to address a major challenge in ischemic stroke (IS) therapy, which is the excessive production of reactive oxygen species (ROS) during reperfusion, which severely damages neurons, combined with the difficulty of delivering drugs across the blood–brain barrier (BBB). To overcome this, the researchers designed a multifunctional nanozyme based on MIL-101-NH_2(Fe/Cu), which served both as a catalytic ROS scavenger and a smart drug delivery platform, and to enhance brain targeting, the nanoparticles were coated with transferrin, which enabled receptor-mediated transport across the BBB and selective accumulation in ischemic brain regions. In a mouse model of middle cerebral artery occlusion/reperfusion, the transferrin-functionalised MOFs demonstrated strong neuroprotective effects by combining antioxidative, anti-inflammatory, and antiapoptotic mechanisms with sustained rapamycin delivery. This synergistic approach significantly reduced infarct volume and improved neurological recovery. These advances highlight how chemical and structural tuning can make MOFs effective tools for treating diseases in difficult-to-reach areas of the body.

After MOFs enter a cell, they undergo endocytosis, where the cell engulfs the particles into small sacs called endosomes. These then merge with lysosomes which are acidic compartments rich in enzymes that break down biomolecules. In this environment, MOFs begin to degrade, releasing their cargo, such as drugs or imaging agents, directly inside the cell[28]. While this is useful for therapy, some MOFs-especially those with redox-active metals like copper-can also release ions that generate reactive oxygen species (ROS), which may damage cells and trigger stress responses[29]. Many metal nodes, particularly redox-active ones such as Fe^{2+}/Fe^{3+}, Cu^{2+}, and Mn^{2+}, can catalyse Fenton or Haber-Weiss type reactions, generating hydroxyl radicals and superoxide anions[24]. Excessive ROS production overwhelms the cell's antioxidant defenses, leading to oxidative stress. This state damages lipids via peroxidation, disrupts membrane integrity, oxidises proteins and enzymes, and induces DNA strand breaks. The cytotoxic potential of MOFs is therefore closely linked to the balance between their ion release and the capacity of the intracellular environment to neutralise ROS. To improve safety and delivery efficiency, researchers have designed MOFs with surface modifications called functionalisations, that help them escape from lysosomes, ensuring the payload reaches the right part of the cell without causing unnecessary cell damage[23].

These examples demonstrate that MOFs are dynamic and responsive materials: their interactions depend heavily on the body's environment, which determines how they behave and how safe they are. The bloodstream, digestive tract, blood-brain barrier, and intracellular compartments each present unique challenges that affect drug delivery, stability, and toxicity. Since a MOF's safety profile is predominantly defined by how it interacts with these environments, understanding these mechanisms is essential before exploring their cytotoxic effects.

CYTOTOXICITY MECHANISMS AND KEY DETERMINANTS

Cytotoxicity is the ability of a substance or material to cause damage to living cells, causing an inhibition of growth, loss of membrane integrity, or cell death[10]. It is a key parameter to measure when assessing the biocompatibility of nanomaterials such as MOFs, particularly when focusing on biomedical applications and clinical use.

MOF induced cytotoxicity can be due to several distinct mechanisms. A key mechanism through which cytotoxicity arises is from oxidative stress, which in turn is caused by the excessive production of reactive oxygen species (ROS) such as O2•-, OH•, OOH•. ROS can be generated by the reaction of transition metal-based nanoparticles with H_2O_2, called the Fenton reaction as shown in Equations (1) and (2)[10]. ROS can also be induced by free radicals present on the reactive surface of nanoparticles as is sometimes observed in functionalised MOFs.

$$Fe^{2+} + H_2O_2 = Fe^{3+} + OH- + OH\bullet \qquad (1)$$

$$Fe^{3+} + H_2O_2 = Fe^{2+} + H^{+} + OOH\bullet \qquad (2)$$

Although a moderate level of ROS is physiologically necessary as it is involved in signal transduction or gene expression, their excessive production may lead to the damage of mitochondrial membranes and also to the proteins, lipids, and mitochondrial DNA found within them. Consequently, it contributes to the activation of inflammation signalling, apoptosis or necrosis[10].

Another observed mechanism of nanoparticle toxicity is endocytosis. Endocytosis itself is one of the cellular uptakes that relies on the penetration of particles into the cell by enclosing them in vacuoles. Phagocytosis, pinocytosis, clathrin and caveolae-mediated endocytosis can be named as the main types of endocytosis[30]. Figure 5 shows the different mechanisms of cellular internalizations of nanoparticles. The

toxicity resulting from this type of uptake is attributed to the free movement of nanoparticles within the cells. For example, MOFs introduced via pinocytosis may distribute in cell membrane, cytoplasm, lipid vesicles, mitochondria, or nucleus[10]. Depending on the localization, they can damage DNA or organelles, and ultimately lead to cell death.

The toxic effect of nanoparticles may also be induced by the cell membrane damage caused by nanoparticles adsorption on the cell surface or due to their diffusion[29]. For instance, Ruenraroengsak et al.[22] showed membrane damage as a mechanism of human alveolar type 1-like epithelial cell death upon exposure to amine modified MOFs. A simplified scheme of the most common mechanisms of MOF induced cytotoxicity is shown in Figure 6.

Recent studies have shown that physico-chemical parameters are the principal determinants of MOF toxicity[30]. Some of the most important factors determining cytotoxicity are (i) metal node chemistry, (ii) organic linker chemistry, (iii) surface functionalisation chemistry, and (iv) particle size and aggregation potential.

Metal node chemistry: The choice of metal node is one of the strongest determinants of a MOF's cytotoxicity profile because it governs both the chemical stability of the framework and the biological activity of released metal ions. MOFs are coordination polymers built from metal nodes (single ions or metal clusters) and organic linkers; under physiological conditions, partial degradation can release these components, exposing cells and tissues to the inherent toxicity of the metal ions. Metals such as Cu^{2+}, Fe^{2+}/Fe^{3+}, Co^{2+}, Mn^{2+}, and Ni^{2+} can participate in redox cycling, generating reactive oxygen species (ROS) through Fenton-like reactions, which leads to oxidative stress, lipid peroxidation, and damage to nucleic acids and proteins[10]. In contrast, Zr^{4+}, Al^{3+}, and Mg^{2+} are considered relatively inert in biological systems, and Zr-based MOFs (e.g., UiO series) are often chosen for biomedical applications because of their high thermodynamic stability and low cytotoxicity[30]. The toxicity of metal ions is therefore not only a function of their intrinsic biological chemistry but also of the coordination environment: strongly bound, high-valent metals in highly stable clusters release fewer ions, whereas labile nodes like Zn^{2+} or Cu^{2+} in certain topologies are more prone to leaching.

Beyond ion release, the structural geometry and surface chemistry of the metal node influence cellular responses. High-valence metal clusters, such as $Zr_6O_4(OH)_4$ nodes, create rigid frameworks with strong metal-ligand bonds that reduce degradation under acidic or enzymatic conditions[7,14,15]. This makes them suitable for drug delivery or imaging applications requiring prolonged circulation. Conversely,

frameworks with softer metal-ligand bonds, like Zn-imidazolate or Cu-carboxylate linkages, are more biodegradable, which can be advantageous for therapeutic payload release but may increase toxicity risk at higher doses. Additionally, certain metal ions exert specific biological effects: Mn^{2+} can mimic essential cofactors but becomes neurotoxic at high intracellular levels, while Fe^{2+}/Fe^{3+} can drive toxicity by promoting lipid peroxidation[10,30]. Even less toxic ions like Mg^{2+} or Ca^{2+} can perturb cellular homeostasis if released in high concentrations, affecting signalling pathways and triggering apoptosis[10,30].

The design of a MOF's metal node thus involves balancing stability and safety with functional requirements such as biodegradability or catalytic activity. Tailoring coordination strength, oxidation state, and surface modification strategies (e.g., polymer coatings or ligand exchange) can significantly mitigate toxicity. Understanding the chemistry of the metal node in physiological conditions is therefore essential for predicting cytotoxicity and for guiding rational MOF design for biomedical applications.

Organic linker chemistry: While the metal node plays a critical role in determining a MOF's chemical stability and toxicity, the organic linker also strongly influences cytotoxicity through its chemical composition, degradability, and interaction with cellular pathways. Organic linkers, typically derived from carboxylates, imidazolates, or other multidentate ligands, can be released as small molecules during MOF degradation. Their intrinsic toxicity depends on factors such as aromaticity, functionalisation, and bioavailability. Aromatic polycarboxylates, for example, are often well tolerated but can still disrupt cellular metabolism at high concentrations, whereas heterocyclic linkers, such as imidazoles, may interfere with enzymatic pathways or induce oxidative stress[10]. Moreover, linker hydrophobicity and charge strongly affect nanoparticle interactions with cell membranes; hydrophobic linkers can promote nonspecific adsorption to lipid bilayers, potentially destabilizing membranes and enhancing cellular uptake[10].

The stability of the linker-metal bond further shapes cytotoxic outcomes. Highly conjugated, rigid linkers tend to form strong coordination bonds with high-valence metals, reducing ion leaching and improving long-term biocompatibility[7,14,15]. Conversely, linkers with pH-sensitive or labile bonds can lead to rapid MOF degradation in acidic compartments like lysosomes, which is useful for drug release but may increase cytotoxicity if ion release is uncontrolled. Thus, linker chemistry directly governs MOF safety profiles by influencing both framework stability and the biological effects of degradation products.

Surface functionalisation chemistry: The chemical modification of linkers or MOF particle surfaces offers a powerful means of controlling MOF interactions with biological systems, and it significantly impacts

toxicity. For example, introducing amino (-NH_2) groups enhances water stability and allows for easier drug loading but can also increase positive surface charge, promoting nonspecific interactions with cell membranes[21,22,30]. Similarly, halogen or hydroxyl substituents influence hydrophobicity and protein corona formation, which alters circulation time and immune recognition[20,21,25]. Surface functionalisation can either mitigate or exacerbate toxicity, depending on how these changes affect biodistribution and degradation kinetics.

Advanced functionalisation strategies, such as PEGylation or coating MOFs with polymers, lipids, or biomolecules, are widely used to enhance colloidal stability, reduce immunogenicity, and improve circulation half-life[11,12,13,15,16,17,18]. These approaches "shield" the framework from rapid opsonization while also slowing degradation, leading to improved safety. Conversely, functional groups designed for targeting-such as folate, peptides, or antibodies-may increase cell-specific uptake, which can amplify cytotoxic effects locally while minimizing systemic toxicity. This tunability makes surface functionalisation a critical design lever for balancing therapeutic efficacy and biocompatibility in MOFs.

Particle size and aggregation potential: Particle size is a critical determinant of a MOF's biological interactions and toxicity, influencing cellular uptake, biodistribution, clearance, and degradation kinetics. Nanometer-scale MOFs (<200 nm) are generally more readily internalised by cells via endocytosis compared to larger particles, which often remain extracellular or are taken up less efficiently[31]. Smaller nanoparticles also have a higher surface area-to-volume ratio, which can accelerate metal ion and linker release, increasing the likelihood of cytotoxic effects through oxidative stress or enzyme disruption[10]. On the other hand, very small MOFs (<50 nm) may penetrate deeper into tissues, cross biological barriers, and accumulate in sensitive organs, raising safety concerns if degradation products are toxic.

Particle size also affects in vivo pharmacokinetics and clearance. Larger particles (>200 nm) are often recognised by the mononuclear phagocyte system and cleared rapidly by the liver and spleen, reducing systemic exposure but potentially causing localised toxicity[18]. Conversely, smaller MOFs are more likely to escape immune clearance and circulate longer, which can improve therapeutic delivery but also increase exposure to healthy tissues. Size tuning is therefore essential to balance drug delivery efficiency with safety.

In addition, aggregation behaviour-which is closely tied to size and surface chemistry-affects biocompatibility. Poorly stabilised MOFs may aggregate in physiological media, altering effective particle size and triggering unintended immune responses or embolism risk[10]. Controlling size distribution and

colloidal stability through synthesis methods, post-synthetic modifications, or polymer/lipid coatings is therefore a key strategy to ensure consistent biological performance. Collectively, particle size is a primary design parameter, influencing not only cytotoxicity but also therapeutic efficacy, circulation time, and tissue targeting.

CYTOTOXICITY MEASUREMENT AND ANALYTICAL METHODS

Evaluating the cytotoxicity of metal-organic frameworks (MOFs) is essential to understanding their biomedical potential and guiding safe material design. Cytotoxicity is commonly measured through dose-response relationships, with indices such as the half-maximal inhibitory concentration (IC_{50}), lethal concentration to 50% of test population (LC_{50}), or cell viability percentages as benchmarks for comparing toxic effects across materials[9,10]. Cytotoxicity profiling typically combines *in vitro* assays, *in vivo* studies, and mechanistic analyses to capture a comprehensive view of how MOFs interact with biological systems.

In vitro cytotoxicity assays: *In vitro* assays are the most widely used first step for screening MOFs. Common methods include (i) 3-(4,5-dimethylthiazol-2-yl)-2,5-diphenyltetrazolium bromide assay (MTT)/ methoxynitrosulfophenyl-tetrazolium carboxanilide (XTT)/ water-soluble tetrazolium salt (WST-1) assays for mitochondrial activity, (ii) LDH release assays for membrane integrity, and (iii) live/dead staining to visualise cell viability[9,10,25]. *In vitro* testing often uses immortalised mammalian cell lines that represent target tissues, such as HeLa (cervical cancer), HepG2 (liver carcinoma), and A549 (lung carcinoma), as well as fibroblast or endothelial cells which allow the assessment of both cancer-specific and normal-cell responses[9,10,25]. Fluorescence or luminescence-based methods allow rapid, high-throughput screening of multiple MOF formulations and concentrations[31]. These assays are inexpensive, reproducible, and provide quantitative toxicity data but may be confounded by optical interference from MOF particles, which can scatter or absorb assay signals[9]. Moreover, in vitro models do not fully capture systemic factors such as protein corona formation, immune clearance, and biodistribution. Advanced in vitro tools include flow cytometry to assess apoptosis and necrosis, ROS quantification assays (e.g., DCFH-DA or 2',7'-dichlorodihydrofluorescein diacetate staining), and high-content imaging to study cell morphology changes. These approaches provide mechanistic insights, but results remain highly cell-line dependent and may not predict in vivo effects accurately[28].

In vivo cytotoxicity testing: Animal models remain the gold standard for evaluating MOF safety profiles. Mouse and zebrafish models are frequently used to study biodistribution, clearance, organ accumulation, and systemic toxicity[10,25,30]. These models can further such insights by recording systemic interactions,

biodistribution, and clearance by using endpoints such as organ-specific toxicity, histopathological evaluation, and survival curves in small-animal studies[24]. However, results from these tests can vary depending on assay type, exposure time, and the biological system employed, which makes the need for careful selection and standardization of cytotoxicity evaluation methods especially crucial when investigating MOFs. Animal testing can also be time-consuming, expensive, and ethically constrained. Additionally, interspecies differences in metabolism and immune function may limit the translation of results to humans[10].

Hemocompatibility and immune interaction tests: Because many MOFs are designed for intravenous delivery, haemolysis assays, coagulation studies, and complement activation tests are critical for assessing compatibility with blood components[32]. These tests measure whether MOFs damage red blood cells, alter clotting cascades, or trigger immune responses. While these studies reveal important information about safety for systemic administration, they are typically performed in simplified systems (e.g., isolated plasma or serum), which may not reflect complex *in vivo* dynamics.

Mechanistic and molecular-level analyses: To better understand how MOFs induce toxicity, mechanistic studies use techniques such as confocal microscopy to track particle internalization, electron microscopy to observe structural interactions, and omics-based approaches (transcriptomics, proteomics, metabolomics) to study cellular responses. These tools have shown, for instance, how MOFs trigger oxidative stress, lysosomal disruption, or ferroptosis pathways[28]. While powerful, these methods require specialised instrumentation and expertise, limiting their accessibility for routine screening.

An integrated strategy that combines these approaches-starting with high-throughput in vitro screening, followed by hemocompatibility assessment, in vivo validation, and mechanistic studies-is essential for building a reliable cytotoxicity profile of MOFs.

RESEARCH OBJECTIVE

Cytotoxicity a central concern in the biomedical application of MOFs, as it becomes both a bottleneck for clinical transition and a necessary focus of safety evaluation. While the overall cytotoxicity profiles of several MOFs are well profiled, the relative contributions of the different components of the MOF to the underlying mechanism for cytotoxic behaviour is relatively poorly understood and is a research gap. An

approach to parse out the contributions to cytotoxic mechanism of the individual components is to study and compare the cytotoxic profile of compositionally related MOFs: frameworks that share a common topology or backbone structure but differ by a single key parameter-such as the metal ion, organic linker, size or a functional group modification. It is observed that even among MOFs that share similar topologies, particle sizes, and porosities, cytotoxicity profiles can vary significantly depending on small changes in their chemistry[3,10,30]. These differences can drastically alter stability, degradation pathways, ion release kinetics, cellular uptake, and ultimately cytotoxic responses of a MOF. By parsing out these individual physico-chemical contributions to cytotoxicity, we can gain better insights into the underlying mechanistic causes.

This literature review was conducted to synthesise current findings on cytotoxicity profiling of compositionally analogous MOFs, with an emphasis on identifying mechanistic explanations for the divergent biological responses exhibited among such structurally similar frameworks. Through integrating evidence from disparate experimental systems and toxicity assays, this paper aims to clarify how minor structural changes can translate into significant changes in cytotoxicity profile and thereby identify trends that can then better guide the design of MOFs for biomedical applications.

MATERIALS AND METHODS

A systematic literature search was conducted across multiple databases, including PubMed, ScienceDirect, JSTOR, ResearchGate, and the Royal Society of Chemistry, covering the period from January 2000 to June 2025. Additional sources were screened through Google Scholar. The search strategy combined controlled vocabulary (MeSH terms) and free-text terms related to metal–organic frameworks (MOFs) and cytotoxicity. For example, a PubMed query used the following structure: (“metal-organic frameworks”[Title/Abstract] OR “MOF”[Title/Abstract] OR “nMOF”[Title/Abstract]) AND (“cytotoxicity”[Title/Abstract] OR “toxicity”[Title/Abstract] OR “biocompatibility”[Title/Abstract]). No language restrictions were applied during the initial screening, although only English-language articles were included in the final analysis.

Studies were considered eligible if they reported experimental cytotoxicity data (*in vitro* or *in vivo*) for at least one MOF, included at least two structurally similar MOFs defined as frameworks with the same topology but differing by a single structural parameter (e.g., metal ion, organic linker, surface

functionalisation, or particle size), and provided sufficient detail for extraction of key cytotoxicity outcomes such as IC_{50} values, LC_{50} values, or cell viability percentages.

All retrieved references were imported into Excel for documentation, where duplicates were removed. Full-text screening was then performed for all potentially eligible studies. Data extraction followed a standardised template and included information on MOF identity (metal node, linker, functionalisation, and particle size), cell line or organism tested, exposure parameters (concentration and incubation time), and key cytotoxicity outcomes. Data were extracted independently, cross-checked for accuracy, and tabulated in Excel.

Given the heterogeneity across experimental models, assay conditions, and cell types, quantitative pooling of results into a meta-analysis was not feasible. Instead, findings were synthesised descriptively and grouped according to compositionally analogous MOFs in which one key physicochemical parameter varied. This approach enabled the identification of trends in cytotoxicity that could be attributed to specific design features, including the choice of metal node, linker chemistry, particle size, or surface functionalisation.

RESULTS AND DISCUSSIONS

Recent studies have shown that physico-chemical parameters are the principal determinants of MOF toxicity[10,30]. In this section the effect of critical physico-chemical parameters such as (i) metal node used in the MOF, (ii) organic linker, (iii) functionalisation, and (iv) particle size is evaluated to assess the effect on MOF toxicity. To gauge the effect of a single physico-chemical parameter on MOF toxicity, compositionally related MOFs are considered for comparison with the principal variant being the parameter under evaluation. The reviewed data is used to create a comprehensive table, in which one can find the overall and relative degree of MOF toxicity affected by the parameter under consideration.

Effect of metal node on MOF cytotoxicity

Metal ions strongly govern MOF toxicity, which has been highlighted in various studies[31,33,34]. Therefore, to design safe MOFs for biomedical applications, the metal choice should be carefully considered. Figure

7 summarises the MOF cytotoxicity comparison of structurally similar MOFs where the primary differentiator is the metal node.

Ruyra et al.[34] studied the cytotoxicity profiles of six MOF-74 analogues with different metal nodes (Mg, Co, Ni, Zn, Mn, Cu), each tested at 200 μM for 72 hours in HepG2 liver carcinoma cells using a cell viability assay. Mg-MOF-74 showed almost complete biocompatibility (96% viability), consistent with the essential role of Mg^{2+} in cellular processes and its lack of redox activity, which minimises reactive oxygen species (ROS) generation[35]. Co-MOF-74, Ni-MOF-74, and Zn-MOF-74 displayed moderate toxicity (68-75% viability), reflecting the biological relevance of these ions but also their ability to interfere with enzymes and protein folding. Excess Zn^{2+}, for instance, can inhibit metabolic enzymes and disrupt signalling pathways[36], while Ni^{2+} and Co^{2+} are known to bind sulfhydryl-containing biomolecules, impairing protein activity and contributing to oxidative stress[37,38]. The most severe effects were observed for Mn-MOF-74 and Cu-MOF-74, with cell viability dropping to 18% and 0%, respectively. Mn^{2+} toxicity arises from its neurotoxic potential and its ability to mimic Ca^{2+}, disrupting calcium-dependent signalling and mitochondrial function, while also contributing to oxidative stress through redox cycling[39]. Cu^{2+}, known for its antimicrobial and cytotoxic properties, readily undergoes redox cycling via the Fenton and Haber-Weiss reactions, generating high levels of ROS that damage lipids, proteins, and DNA[40,41]. Overall, the results highlight a clear trend of increasing cytotoxicity with transition metals of higher redox activity.

Tamames-Tabar et al.[42] evaluated the cytotoxicity of MIL-88B (Fe-based) and UiO-66 (Zr-based) nanoparticles (~100 nm) in two distinct cell types: J774 macrophages and HeLa epithelial cells. In J774 cells, UiO-66 demonstrated a significantly lower IC_{50} (60 μg/mL) than MIL-88B (370 μg/mL), indicating higher toxicity under identical conditions. A similar pattern was observed in HeLa cells, where UiO-66 exhibited an IC_{50} of 400 μg/mL, compared to 1260 μg/mL for MIL-88B. These results highlight UiO-66's greater cytotoxicity across both immune and epithelial models, despite Zr^{4+} being considered chemically inert[7,14,15]. This difference suggests that framework structure, surface chemistry, and defect density could contribute to toxicity outcomes. UiO-66's defect-tolerant, high-surface-area structure may facilitate interactions with cellular membranes or lead to faster linker release under acidic intracellular conditions, particularly in phagocytic cells like J774 macrophages[43]. In contrast, MIL-88B's flexible, iron-based framework appears comparatively less cytotoxic, which may reflect slower degradation kinetics and differences in stability[28]. This dataset suggests that framework characteristics could also be important in shaping MOF toxicity in addition to the metal characteristics.

Yang et al.[44] evaluated the in vivo toxicity of three widely studied MOFs-MIL-101(Fe)-NH_2, UiO-66-NH_2, and HKUST-1-using zebrafish embryo models over a 96-hour exposure period. The findings demonstrate clear differences in toxicity that strongly correlate with metal node chemistry and framework stability. Both MIL-101(Fe)-NH_2 and UiO-66-NH_2 exhibited LC_{50} values greater than 400 μg/mL, indicating high biocompatibility and stability under biological conditions likely due to the relative inertness of Fe^{3+} and Zr^{4+}. By contrast, HKUST-1 showed severe toxicity with an LC_{50} of 1.97 μg/mL, underscoring the risks posed by copper-based MOFs. Copper's strong redox activity and HKUST-1's moderate aqueous stability are known to facilitate rapid Cu^{2+} release, leading to oxidative stress, mitochondrial dysfunction, and membrane damage as discussed earlier. These results suggest while Fe- and Zr-based MOFs appear well-tolerated, Cu-based frameworks like HKUST-1 exhibit higher toxicity levels limiting their suitability for systemic biomedical use.

Zhang et al.[45] evaluated the cytotoxicity of UiO-66 (Zr-based) and HKUST-1 (Cu-based) nanoparticles (30-100 nm) in human bronchial epithelial cells (BEAS-2B) following 24-hour exposure at 200 μg/mL. UiO-66 showed high biocompatibility, maintaining 90% cell viability, consistent with previous findings that Zr-based MOFs are generally stable and inert in biological environments[7,14,15]. In contrast, HKUST-1 demonstrated severe toxicity, with viability dropping to 10%, reinforcing copper's well-documented redox activity and tendency to catalyse reactive oxygen species (ROS) generation leading to lipid peroxidation, mitochondrial dysfunction, and apoptosis, as discussed earlier. These findings corroborate trends observed in zebrafish and other cell lines, where HKUST-1 exhibited high toxicity, while UiO-66 maintains low cytotoxicity. The consistency across models strengthens the evidence that metal node selection plays a dominant role in MOF safety: Zr-based frameworks remain promising for biomedical applications, while Cu-based frameworks pose safety concerns for systemic delivery.

Sifaoui et al.[46] investigated the cytotoxicity of several CIM-series MOFs and UiO-66 in J774 macrophage cells after 24-hour in vitro exposure. The results reveal a distinct separation between biocompatible frameworks and moderately toxic Zn-based frameworks. CIM-80 (Al-based), CIM-84 (Zr-based), and UiO-66 (Zr-based) exhibited LC_{50} values above 5000 μg/mL, indicating good tolerance and minimal cytotoxicity. These findings are consistent with prior evidence of Al^{3+} and Zr^{4+} frameworks being chemically inert, structurally stable, and resistant to rapid ion release. By contrast, CIM-81 and CIM-91, both Zn-based frameworks containing 1,2,4-triazole and terephthalate linkers, showed LC_{50} values of 980 μg/mL and 880 μg/mL, respectively. Although still relatively safe compared to Cu-based frameworks like HKUST-1, these values suggest that Zn^{2+} frameworks exhibit moderate cytotoxicity, likely due to higher

ion solubility and interaction with intracellular enzymes[30]. Overall, these findings reinforce that Al- and Zr-based frameworks demonstrate good safety, whereas Zn-based frameworks, though generally biocompatible, exhibit higher cytotoxicity.

Grall et al.[47] assessed the cytotoxicity of MIL-100 frameworks incorporating Fe^{3+}, Al^{3+}, and Cr^{3+} nodes, all synthesised with benzene-1,3,5-tricarboxylate (BTC) linkers, in A549 lung epithelial cells and Hep3B liver carcinoma cells. All MOFs were tested at a dose of 64 μg/cm² for 24 hours. In A549 cells, all variants exhibited good biocompatibility, with cell viabilities of 95% (Fe), 97% (Al), and 99% (Cr), indicating negligible cytotoxicity. However, in Hep3B cells, the Fe-based MOF showed lower viability (60%) than its Al (80%) and Cr (82%) counterparts, suggesting a cell-type-specific sensitivity likely tied to liver cell metabolism and iron handling. The improved tolerance of Al- and Cr-based MIL-100 frameworks may be attributed to their greater thermodynamic stability and the lower biological reactivity of Al^{3+} and Cr^{3+} ions compared to Fe^{3+}. Iron is tightly regulated in mammalian systems due to its participation in Fenton chemistry, where free Fe^{2+}/Fe^{3+} can catalyse the formation of highly reactive hydroxyl radicals, potentially increasing oxidative stress when iron is released[39]. In contrast, Al^{3+} is redox-inactive, and Cr^{3+}, while a transition metal, has low solubility and minimal redox activity at physiological pH[38]. These properties likely result in slower degradation kinetics and less oxidative stress induction, explaining their higher cell viability outcomes. Overall, these findings reinforce that metal node redox potential and ion speciation play crucial roles in MOF cytotoxicity: Fe-based frameworks may be more prone to ROS generation in metabolically active cells like hepatocytes, while Al- and Cr-based MIL-100 maintain better safety profiles.

In summary, the above evidence across multiple studies demonstrates that the metal node is an important factor driving cytotoxicity in structurally similar MOFs, with redox activity, ion release dynamics, and cellular handling of specific metals shaping toxicity outcomes. Cu^{2+}-based frameworks such as HKUST-1 consistently exhibit the highest toxicity, likely due to copper's strong redox cycling, which generates ROS and induces mitochondrial damage, lipid peroxidation, and apoptosis. Mn^{2+} frameworks also rank highly toxic, reflecting their ability to mimic Ca^{2+}, disrupt calcium signalling, and promote oxidative stress. Zn^{2+}-based MOFs show moderate toxicity, linked to zinc's higher solubility and enzyme-inhibiting properties, whereas Fe^{3+}-based frameworks are variably tolerated; although stable, iron can catalyse ROS via Fenton chemistry, particularly in metabolically active liver cells. In contrast, Cr^{3+}, Al^{3+}, and Zr^{4+} frameworks demonstrate good biocompatibility, supported by their low solubility, chemical inertness, and resistance to rapid degradation. This establishes a general toxicity ranking of Cu and Mn having relatively

higher toxicity, Fe, Zn, Co, Ni, Mg with moderate toxicity and Cr, Al and Zr having better biocompatibility (Figure 8). Together, these results emphasise that careful selection of redox-inactive metals such as Zr or Al is important for designing MOFs for biomedical applications, while redox-active metals like Cu and Mn may be used for antimicrobial or anticancer therapies where cytotoxicity is desired.

Effect of organic linker on MOF cytotoxicity

Linker chemistry is also an important determinant of MOF cytotoxicity. Figure 9 summarises the MOF cytotoxicity comparison of compositionally related MOFs where the primary differentiator is the organic linker.

Tamames-Tabar et al.[42] investigated the cytotoxicity of four Fe-based MOFs-MIL-100(Fe), MIL-127, MIL-88B, and MIL-88A-alongside their organic linkers, in both J774 macrophage and HeLa epithelial cell lines. This dataset provides insight into how linker chemistry influences MOF toxicity independently of the metal node. MIL-100(Fe), constructed from trimesic acid (H_3BTC), exhibited low cytotoxicity in both cell types, with IC_{50} values of 700 μg/mL in J774 and 1100 μg/mL in HeLa, while its linker also showed minimal toxicity (>1000-2000 μg/mL). This reflects the high stability and low reactivity of trimesic acid linkers, which reduce ion release and cellular stress. In contrast, MIL-127, built from a tetrazolate-benzene (Tazb) linker, showed moderate toxicity in J774 macrophages (IC_{50} 440 μg/mL) but high tolerance in HeLa cells (>2000 μg/mL). Its linker IC_{50} values (820 μg/mL in J774; 800 μg/mL in HeLa) suggest that the polar tetrazolate functionality contributes to good water stability, potentially slowing degradation. The comparatively higher macrophage toxicity may also relate to particle size (476 nm), which facilitates phagocytosis[42]. MIL-88B, incorporating terephthalic acid (H_2BDC), showed moderate toxicity (IC_{50} 370 μg/mL in J774; 1260 μg/mL in HeLa) consistent with its linker toxicity (430 μg/mL in J774; 800 μg/mL in HeLa), reflecting the aromatic structure and lower solubility of BDC. MIL-88B's flexible structure likely enables faster degradation, releasing both Fe^{3+} and BDC, producing cell-specific effects. On the other hand, MIL-88A, based on fumaric acid (FUM), was highly toxic, with IC_{50} values of 50 μg/mL in J774 and 15 μg/mL in HeLa, much lower than its isolated linker (400 μg/mL in J774; 30 μg/mL in HeLa). This discrepancy suggests synergistic toxicity driven by rapid degradation, as fumaric acid is highly hydrophilic and easily exchanged in aqueous environments, accelerating Fe^{3+} release and enhancing oxidative stress[48].

Recent findings by Liu et al.[49] reinforce the important role of the organic linker in MOF cytotoxicity. In A549 lung epithelial cells exposed for 24 hours at 100 μg/mL, MIL-101(Fe) (terephthalate, H_2BDC linker) maintained 58% cell viability, consistent with previous studies demonstrating moderate cytotoxicity and relative framework stability of Fe-BDC materials. In contrast, MIL-88A (Fe-fumarate) of comparable size (~1.1 μm) showed severe cytotoxicity, with viability dropping to 10% under identical conditions. This sharp difference supports earlier observations that fumarate-based MIL-88A degrades more rapidly in biological environments due to the hydrophilic and highly accessible fumarate linkers, which facilitate faster Fe^{3+} release and subsequent ROS generation. The pronounced toxicity of MIL-88A aligns with its known flexible, rod-like structure that undergoes structural collapse and hydrolysis in aqueous and phosphate-buffered media, triggering metal ion release and oxidative stress[34,50]. By contrast, MIL-101's larger, more robust BDC-based framework resists linker exchange and ion release, explaining its lower cytotoxicity.

The study by Yang et al.[44] looks at linker-toxicity analysis in an *in vivo* zebrafish embryo model, comparing ZIF-8 (Zn-MIM) and ZIF-90 (Zn-HICA) over a 96-hour exposure period. ZIF-8 exhibited a relatively high LC_{50} of 143.47 μg/mL, indicating moderate toxicity, whereas ZIF-90 showed a much lower LC_{50} of 19.61 μg/mL, reflecting severe toxicity. Although both frameworks share a Zn^{2+} node and similar topologies, their linkers differ in polarity and chemical reactivity: ZIF-90's aldehyde group in HICA introduces greater hydrophilicity and electrophilic reactivity, which likely accelerates framework dissolution and enhances interaction with biological molecules, increasing Zn^{2+} release and oxidative stress. In contrast, ZIF-8's methyl-substituted MIM linker imparts higher hydrophobicity and relative stability, resulting in reduced toxicity. These results highlight that linker functionalisation can significantly alter biological interactions and stability, even in topologically similar frameworks, reinforcing that linker selection is a critical factor for predicting MOF safety profiles.

Finally, Ruyra et al.[34] evaluated cytotoxicity in structurally similar MOFs with four different metal nodes - Cu, Zr, Fe and Zn. Among copper-based MOFs, both HKUST-1 (Cu-H_3BTC) and NOTT-100 (Cu-BPTC) exhibited severe toxicity in HepG2 cells after 72 hours at 200 μM, with cell viabilities of 0% and 5%, respectively. Although their free linkers were only moderately cytotoxic (79-85% viability), the frameworks themselves were dramatically more toxic, underscoring that Cu^{2+} release and redox activity dominate toxicity in these systems. Minor differences in toxicity between HKUST-1 and NOTT-100 may reflect differences in linker geometry and hydrophobicity, which influence framework stability and metal ion leaching. A strong contrast is observed with Zr-based frameworks, which remained highly

biocompatible regardless of linker choice. Both UiO-66 (Zr-BDC) and UiO-67 (Zr-BPDC) maintained 96-98% viability, closely matching the cytotoxicity profiles of their respective linkers (85-95% viability). These results demonstrate that the exceptional stability of Zr-O coordination bonds and low solubility of Zr^{4+} largely decouple linker chemistry from overall toxicity outcomes. For Fe-based frameworks, linker identity exerts a stronger influence. MIL-100 (Fe-BTC) displayed 80% viability, while MIL-101 (Fe-BDC) dropped sharply to 45% viability, despite similar linker toxicities (~79-81% viability). This disparity suggests that differences in framework architecture and degradation profile can amplify toxicity when paired with Fe^{3+} nodes. The higher surface area and flexible pore structure of MIL-101 may promote faster dissolution, enhancing Fe^{3+} release and ROS generation. Finally, Zn-based ZIFs highlight how subtle linker changes can significantly alter biological responses. ZIF-7 (Zn-BIM) retained 85% viability, whereas ZIF-8 (Zn-MIM) showed a sharp reduction to 40% viability under identical conditions. This contrast reflects the influence of methylation in the MIM linker, which increases hydrophobicity and affects framework solubility, accelerating Zn^{2+} release and cytotoxic effects.

From the above comparative studies across different datasets, it was found that organic linker chemistry plays a key role in shaping MOF toxicity, influencing framework stability, degradation kinetics, and biological interactions. Hydrophilic and reactive linkers such as fumarate (MIL-88A) and HICA (ZIF-90) correlate with higher cytotoxicity, as their polarity and small size facilitate rapid hydrolytic degradation and metal ion release, resulting in ROS generation and mitochondrial stress. Methylimidazolate (MIM) in ZIF-8 exhibits moderate toxicity, with its hydrophobicity providing relative stability, while tetrazolate-benzene (Tazb) in MIL-127 shows similar mid-range cytotoxicity (~440-820 μg/mL), reflecting the polar, heterocyclic tetrazole group that enhances water. Benzene-based linkers such as BDC (terephthalate) and BTC (trimesate) are generally well tolerated, contributing to good biocompatibility in frameworks like UiO-66 and MIL-100. Notably, although BTC is hydrophilic due to its three carboxylate groups, it forms rigid, multi-connected 3D networks (e.g., HKUST-1, MIL-100) that resist ligand exchange, limiting degradation[51,52]. In contrast, fumarate's ditopic geometry and small size favor flexible topologies like MIL-88A, accelerating hydrolysis and increasing toxicity. Larger, rigid linkers such as BPDC further enhance stability, as seen in UiO-67, which remained highly biocompatible across systems. Overall, this establishes a relative toxicity ranking of HICA ≈ fumarate > MIM ≈ Tazb > BDC ≈ BTC ≈ BPDC, with linker polarity, size, functional group reactivity, and network rigidity being key determinants (Figure 10).

However, metal node identity can override linker effects, as demonstrated in Ruyra et al.[34], where Cu-based frameworks (HKUST-1, NOTT-100) caused nearly complete cell death despite their linkers being moderately biocompatible, emphasizing that Cu^{2+}'s strong redox activity and rapid leaching dominate toxicity outcomes. Conversely, Zr-based frameworks remained highly stable regardless of linker chemistry, underscoring that high-valence, inert metals like Zr^{4+} dampen linker contributions to toxicity. These findings indicate that while linker design strongly influences MOF degradation and cellular interactions, metal node selection is the primary determinant of overall safety, with redox-active metals amplifying cytotoxic effects and inert metals offering a stable platform for biomedical applications. For rational MOF design, linker hydrophilicity, degradation potential and chemical reactivity must be tuned with the chosen metal node to optimise both stability and biocompatibility.

Effect of functionalisation on MOF cytotoxicity

MOFs are often functionalised to fine-tune their surface chemistry, pore environment, and stability for specific applications such as catalysis, gas storage, sensing, and biomedical use. By introducing functional groups, one can control hydrophilicity, enhance chemical stability, create selective binding sites, or improve biocompatibility, making them more specific for its intended application. Figure 11 summarises the MOF cytotoxicity comparison of compositionally related MOFs where the primary differentiator is the surface functionalisation.

Tamames-Tabar et al.[42] investigated how surface functionalisation affects the cytotoxicity of two iron-based MOFs, MIL-101 and MIL-88B, both of which share the terephthalate (H_2BDC) linker but differ in framework flexibility - MIL-101 being more rigid with permanent large pores and high stability and MIL-88B being more flexible whose pore size and shape change dynamically with its chemical environment. Across both MOFs, cytotoxicity was quantified by IC_{50} values (μg/mL) in HeLa epithelial cells and J774 macrophages after 24-hour exposure, allowing direct comparison of different surface groups, including $-NH_2$, $-CH_3$, $-NO_2$, $-CF_3$, and unmodified (-H) MOFs.

For MIL-101, functionalisation strongly influenced biocompatibility, especially in immune cells. In HeLa cells, methyl-functionalised MIL-101(Fe)_$2CH_3$ demonstrated excellent tolerance (IC_{50} > 2500 μg/mL), followed by amino-functionalised MIL-101_NH_2 (IC_{50} > 1000 μg/mL). However, macrophages showed heightened sensitivity: IC_{50} values decreased to 170 μg/mL for the methyl variant and 70 μg/mL for the

amino variant, underscoring cell-type-dependent effects and macrophages' greater susceptibility to nanoparticle-induced stress. The polar -NH_2 functionality exhibited greater toxicity than nonpolar -CH_3 in J774 cells, possibly due to NH_2 being protonated to NH_3^+ under physiological conditions and the positive surface charge can lead to membrane adhesion and uptake, which can trigger ROS generation within the cell leading to cytotoxicity[40].

For MIL-88B, the trends were more complex, reflecting this framework's flexibility and smaller particle size. In HeLa cells, NO_2- and CF_3-functionalised MIL-88B variants were the least toxic (IC_{50} > 2000 μg/mL), while tetra-methyl substitution (MIL-88B_4CH_3) lowered IC_{50} to 690 μg/mL, suggesting that excessive hydrophobic modification may promote aggregation or destabilise interactions with membranes. In J774 macrophages, NO_2 substitution dramatically increased toxicity (IC_{50} = 30 μg/mL), while tetra-methyl substitution also caused a sharp reduction in IC_{50} to 80 μg/mL, indicating that immune cells are highly sensitive to both strongly electron-withdrawing and heavily hydrophobic surface chemistries. In contrast, singly or doubly methylated variants (MIL-88B_CH_3 and MIL-88B_2CH_3) retained moderate cytotoxicity (IC_{50} ≈ 360-370 μg/mL), while the unmodified framework remained relatively safe (IC_{50} = 370 μg/mL).

Ruyra et al.[34] provided a direct comparison of standalone UiO-66 and its amino-functionalised analogue UiO-66-NH_2, both constructed from Zr^{4+} nodes and terephthalate linkers, to evaluate the specific impact of -NH_2 substitution on cytotoxicity. When tested in HepG2 liver carcinoma cells at 200 μM for 72 h, pristine UiO-66 maintained very high cell viability (96%), consistent with the known biocompatibility of Zr-based MOFs due to their high thermodynamic stability and slow degradation in biological media. The introduction of amino groups modestly reduced viability to 75%, indicating that surface polarity and hydrogen-bonding capacity can enhance interactions with proteins and cellular membranes, potentially increasing particle uptake and ROS generation as in the earlier study.

Overall, these datasets demonstrate that surface chemistry significantly modulates MOF toxicity in a cell-type-dependent manner, with macrophages being significantly more sensitive to certain functionalities. Polar (-NH_2) and electron-withdrawing substituents (-NO_2) appear to enhance interactions with immune cells, while bulky hydrophobic groups (tetra-CH_3) may promote aggregation and alter biodistribution, both leading to higher toxicity. Milder substitutions (mono-/di-CH_3) and CF_3 appear less cytotoxic in epithelial models. These results highlight the need to optimise surface functionalisation based on target cell types, balancing hydrophilicity, charge, and steric effects to minimise adverse outcomes.

Effect of MOF particle size on cytotoxicity

The size of the nanoparticles can also meaningfully influence the cytotoxicity profile of the MOF. As the particle size decreases, its ability to pass through physiological barriers increases thereby increasing its likelihood to cause cellular damage. Smaller particles also expose a larger surface area to their microenvironment and diffusion is also much faster, typically resulting in a faster degradation for a given MOF, which can also increase the likelihood of cellular damage[30]. Figure 12 summarises the study comparisons where particle size is the key variable.

Liu et al.[49] investigated size-dependent cytotoxicity using two Fe-based MOFs-MIL-101(Fe) (H_2BDC linker, rigid mesoporous framework) and MIL-88A (fumarate linker, breathing framework)-in A549 lung epithelial cells exposed to 100 μg/mL for 24 h. For MIL-101(Fe), smaller nanoparticles (~236 nm) showed higher cytotoxicity (42% cell viability) than their larger counterparts (~487 nm: 52%, ~968 nm: 54%), consistent with expectations that nanosized MOFs possess greater reactive surface area and dissolve more rapidly in biological media, leading to faster Fe^{3+} release and oxidative stress. In contrast, MIL-88A, a more flexible, breathing MOF, demonstrated an even sharper size-toxicity relationship: the smallest particles (~1.1 μm) caused severe cytotoxicity (9% viability), whereas much larger particles (~3.5 μm and ~4.9 μm) were progressively less toxic (22% and 45% viability, respectively). These findings emphasise that nanoscale particles (sub-micron) are more readily internalised by epithelial cells via clathrin- and caveolin-mediated endocytosis, whereas microparticles above ~2-3 μm face reduced uptake, resulting in lower intracellular ion release and toxicity[53,54].

Mechanistically, two synergistic factors explain the observed trends: (1) Surface area and dissolution kinetics-smaller MOFs present higher surface area-to-volume ratios, accelerating linker hydrolysis and Fe^{3+} release in acidic lysosomes, which drives reactive oxygen species (ROS) production and cell stress; (2) Endocytic uptake thresholds-particles in the 50-500 nm range are optimal for endocytosis, while particles >1-2 μm are less efficiently internalised, thus limiting intracellular exposure[55]. Framework flexibility adds complexity: MIL-88A's breathing structure may undergo additional pore collapse or dynamic changes upon cellular entry, amplifying the cytotoxic effects of small particles. Together, these data highlight the importance of size engineering in designing MOFs for biomedical applications: while nanoscale MOFs enable higher cellular delivery, they also pose increased toxicity risks, particularly for redox-active metal nodes like Fe^{3+}.

Chen et al.[56] conducted an evaluation of particle size effects in ZIF-8 nanoparticles, holding chemical composition constant while varying particle diameters between 50, 90, and 200 nm. Cytotoxicity assays in HepG2 liver carcinoma cells revealed a clear inverse size-toxicity trend: the smallest particles (50 nm) showed the highest toxicity with an IC_{50} of 15.6 μg/mL, while larger particles of 90 and 200 nm showed progressively higher IC_{50} values of 17.5 and 19.7 μg/mL, respectively. These findings align closely with Liu et al.[49], who demonstrated a similar trend in Fe-based MIL-101 and MIL-88A MOFs, where smaller nanoparticles were consistently more cytotoxic due to their higher surface reactivity and more efficient endocytic uptake. Together, these results reinforce that size reduction, particularly into the sub-100 nm range, amplifies toxicity risks across different MOF chemistries by accelerating ion release kinetics and intracellular exposure.

Hao et al.[57] examined the effect of particle size on cytotoxicity in PCN-224, a Zr-based porphyrinic MOF constructed from tetrakis(4-carboxyphenyl)porphyrin (TCPP) linkers. Nanoparticles of 30, 90, and 180 nm were tested in J774 macrophages, showing a pronounced inverse size-toxicity trend. The smallest particles (30 nm) exhibited the highest cytotoxicity ($IC_{50} \approx 35$ nM), while larger 90 nm and 180 nm particles had progressively higher IC_{50} values of 50 nM and 100 nM, respectively, reflecting reduced potency with increasing size. These findings are consistent with observations from Liu et al.[49] and Chen et al.[56], confirming that nanoscale MOFs below ~100 nm present heightened toxicity risks across diverse chemistries and cell types. The macrophage model highlights a key mechanistic factor: phagocytes like J774 cells internalise nanoparticles very efficiently, particularly when they are in the 20-100 nm range, leading to increased intracellular exposure, lysosomal degradation, and metal ion release even for highly stable Zr frameworks. This work reinforces the general principle that smaller particles provide high cellular delivery efficiency but increase cytotoxic potential, emphasizing the need for careful size tuning in biomedical MOF design.

Zhu et al.[58] investigated the cytotoxicity of Mg-MOF-74 with two distinct particle sizes-nanoscale (~300 nm) and microscale (~3.7 μm)-in J774 macrophages. Interestingly, this study demonstrated a reversal of the typical size-toxicity trend observed in other MOFs: the nanoscale material exhibited very low toxicity ($IC_{50} > 2000$ μg/mL), while the larger microparticles showed a substantially lower IC_{50} of 798 μg/mL, indicating higher cytotoxicity. This inverse relationship is likely due to the mechanical stress when attempting to internalise large particles (>2-3 μm), which can trigger inflammatory responses and cell damage independent of chemical dissolution[44]. This finding highlights that while nanoscale particles

generally pose higher toxicity risks via enhanced uptake and ion release, very large MOF crystals introduce size-specific mechanical effects that can dominate cellular outcomes at the micron scale.

Jiang et al.[59] examined the cytotoxicity of Bio-MOF-1, a zinc-based adenine and BPDC framework, in nanoscale (~594 nm) and extremely large microscale (~65.8 μm) crystals in MC3T3-E1 osteoblastic cells. The trend mirrored that of Zhu et al.[58], where the microscale particles exhibited significantly higher cytotoxicity (IC_{50} 248 μg/mL) compared to the nanoscale sample (IC_{50} 599 μg/mL). This effect is likely due to mechanical stress and impaired cellular handling of very large particles, which macrophages and other cells struggle to internalise, potentially leading to membrane disruption and inflammatory signalling. Similar to the findings in Mg-MOF-74, these results emphasise that once particle size exceeds several microns, mechanical effects may outweigh traditional nanoparticle toxicity mechanisms, such as ion release or reactive oxygen species (ROS) generation.

Across multiple studies, particle size emerges as a critical determinant of MOF cytotoxicity, with a general trend of increasing toxicity as size decreases into the nanoscale range, but notable exceptions at extreme microscale sizes. In Fe-based MIL-101 and MIL-88A[49], ZIF-8[57], and Zr-porphyrinic PCN-224[50], smaller nanoparticles consistently exhibited higher cytotoxicity, driven by their high surface area-to-volume ratios, faster ion release kinetics, and more efficient uptake via clathrin- and caveolin-mediated endocytosis. This effect was most pronounced for sub-100 nm ZIF-8 particles, where IC_{50} values dropped sharply, highlighting the elevated risk associated with ultra-small particles. However, studies on Mg-MOF-74[58] and Bio-MOF-1[59] revealed that at extreme microparticle sizes (>3-5 μm), toxicity can rise again, likely due to mechanical stress as cells struggle to engulf oversized particles, triggering membrane damage and inflammatory responses[46]. Together, these findings suggest a U-shaped relationship between size and toxicity: toxicity is high for very small nanoparticles (<200 nm) due to rapid cellular internalization and dissolution, moderate for mid-sized particles (~500-2000 nm) where uptake and dissolution are balanced, and high again for very large microparticles (>5 μm) due to physical stress on cells. Framework flexibility further modulates these effects, as seen in MIL-88A, where breathing behaviour amplified cytotoxicity at smaller sizes. This integrated evidence underscores the importance of precise size engineering for biomedical MOFs: particles in the intermediate size range (~200-1000 nm) may offer the best compromise between cellular uptake and biocompatibility, whereas very small or very large sizes introduce distinct toxicity risks through chemical and mechanical mechanisms, respectively.

Taken together, these findings highlight that MOF cytotoxicity is driven by a complex interplay between metal node composition, linker and surface chemistry, and particle size rather than any single factor.

The metal node is a dominant determinant of MOF cytotoxicity, with redox activity, ion release rates, and biological handling of specific ions strongly shaping toxicity. Cu^{2+}- and Mn^{2+}-based frameworks consistently exhibit high toxicity, largely due to redox cycling and disruption of calcium signalling, while Zn^{2+} and Fe^{3+} frameworks show moderate toxicity, reflecting their greater solubility and potential for ROS generation. In contrast, Al^{3+}, Cr^{3+}, and Zr^{4+} frameworks demonstrate excellent stability and low cytotoxicity, supported by their redox-inert chemistry and resistance to rapid degradation. Across studies, metal node choice frequently overrides other variables, providing a clear hierarchy: Cu ≈ Mn > Zn ≈ Fe > Co ≈ Ni ≈ Mg > Al ≈ Cr ≈ Zr. This underlines that selecting inert metals such as Zr or Al is essential for safe biomedical applications, while Cu or Mn nodes may be exploited for antimicrobial or anticancer activity.

Linker identity shapes cytotoxicity primarily by influencing framework degradation kinetics, ion release, and membrane interactions. Hydrophilic or reactive linkers (fumarate, HICA) drive rapid hydrolysis and heightened toxicity, while aromatic, rigid linkers such as BTC, BDC, and BPDC contribute to structural stability and biocompatibility. Subtle changes, like methylation of imidazoles in ZIF-8, also modulate solubility and Zn^{2+} release. Although linker chemistry is highly influential, its effect is strongly modulated by metal identity: Zr frameworks remained nontoxic regardless of linker, whereas Cu frameworks were toxic even with benign linkers. The data establish a toxicity trend of HICA ≈ fumarate > MIM ≈ Tazb > BDC ≈ BTC ≈ BPDC.

Surface chemistry fine-tunes MOF toxicity, with polar or electron-withdrawing substituents ($-NH_2$, $-NO_2$) often increasing toxicity via enhanced uptake and ROS generation, especially in macrophages. Hydrophobic functionalisation (multi-CH_3) may induce aggregation, leading to variable cytotoxicity, while moderate substitutions or CF_3 groups are relatively safe. Functionalisation effects are cell-type-specific, demonstrating the need for targeted engineering.

Particle size exerts a U-shaped effect on toxicity. Nanoparticles <100-200 nm increase cytotoxicity via high surface reactivity and efficient endocytic uptake, while very large microparticles (>3-5 μm) induce toxicity through mechanical stress and inflammatory signalling. Mid-sized particles (~200-1000 nm) appear to offer a balance of cellular delivery and biocompatibility. Framework flexibility amplifies these size effects, as seen in MIL-88A's breathing structure.

Despite the clear structure–toxicity trends established in this review, certain methodological limitations inherent to the primary literature must be acknowledged. Cytotoxicity studies on MOFs show considerable heterogeneity in their experimental designs, including variations in exposure duration, biological models, assay types, and the cytotoxicity indices used (for example, IC_{50} versus LC_{50} versus cell viability percentages). A further challenge in evaluating MOF cytotoxicity lies in the inconsistent use of toxicity units across the literature. Some studies report concentration-based endpoints (μg/mL), while others use molar units (μM) or viability percentages. These indices are not directly interchangeable, as they depend on molecular weight, assay sensitivity, and cellular context. This heterogeneity complicates direct cross-study comparisons and the establishment of universal toxicity rankings. To mitigate this issue, the present analysis was deliberately restricted to within-study comparisons of structurally similar or compositionally related frameworks, thereby controlling for inter-assay variability and methodological bias. Nevertheless, the lack of standardised testing protocols across MOF toxicology remains a major challenge in the field, underscoring the need for harmonised assay conditions and consistent reporting formats to enable more quantitative comparisons in future studies.

CONCLUSIONS

This review highlights that minor structural variations among MOFs-including metal node, linker, functionalisation, and particle size-can dramatically alter cytotoxic profiles, even when frameworks share identical topology. The dominant factor is the metal node, which dictates degradation kinetics and ion toxicity, with Zr and Al nodes consistently demonstrating high stability and low toxicity, while Cu and Mn nodes pose higher risks. Organic linkers further modulate toxicity, with hydrophilic, labile linkers accelerating degradation, while rigid, aromatic linkers confer stability. Functionalisation fine-tunes these effects, where polar or charged groups promote uptake but may increase ROS generation, whereas neutral groups improve biocompatibility. Particle size exerts a dual influence: nanoparticles enhance cellular internalization and dissolution-driven toxicity, while oversized microparticles induce mechanical stress. Collectively, these findings provide a mechanistic framework for designing MOFs with optimised safety, underscoring the importance of balancing metal-ligand stability, linker chemistry, surface modification, and size control.

LIMITATIONS AND FUTURE RECOMMENDATIONS

Limitations

While this review synthesises extensive data on the cytotoxicity of compositionally analogous MOFs, following are some of the limitations of this study. First, the heterogeneity of study designs-including variations in cell lines, assay types, exposure times, and endpoints (IC_{50} vs. LC_{50} vs. cell viability percentages)-limits direct cross-comparison of toxicity values. Second, the physicochemical properties of MOFs, such as particle size, agglomeration, surface chemistry, and crystallinity, are often reported inconsistently, making it difficult to fully decouple single variables from other confounding factors. Third, most of the available studies rely on *in vitro* data, which, while useful for screening, cannot fully capture the complexity of in vivo biodistribution, immune response, and long-term toxicity. Furthermore, most studies do not fully examine how MOFs degrade in the body or how their released precursor metal ions, linkers or functional groups behave, yet these processes largely determine their actual toxicity.

Future recommendations

To further the safe and rational design of MOFs for biomedical use, following research directions are recommended:

1. **Standardization of Testing Protocols**
   Development of standardised cytotoxicity evaluation guidelines for MOFs-including cell panel selection, assay combinations, dose-time profiles, and reporting metrics-would allow for more meaningful comparisons across studies.
2. **Mechanistic Toxicology Studies**
   Detailed mechanistic investigations linking metal ion, linker, functional group release profile, ROS generation pathways, and calcium signaling disruption to cellular outcomes are essential to understanding the cytotoxicity profile.
3. **Integrated In Vitro-In Vivo Models**
   Bridging *in vitro* testing with physiologically relevant *in vivo* studies, such as zebrafish or murine models, will provide more accurate predictions of biodistribution, clearance, and systemic toxicity.
4. **Long-Term and Chronic Exposure Studies**
   Investigating chronic exposure, bioaccumulation, and toxicity is critical to evaluating the long-term safety of MOFs, particularly for repeat-dose drug delivery or implantable device applications.

ACKNOWLEDGEMENTS

I would like to express my sincere gratitude to Dr. Francesca Melle, Department of Chemical Engineering and Researcher at the Adsorption and Advanced Materials Laboratory at the University of Cambridge for her insightful guidance and invaluable feedback throughout this research.

CONFLICTS OF INTEREST

The author declares that there are no conflict of interests related to this work.

REFERENCES

1. Yaghi, O., Li, G. & Li, H. Selective binding and removal of guests in a microporous metal-organic framework. *Nature* 378, 703-706 (1995). https://doi.org/10.1038/378703a0

2. Horcajada, P., Chalati, T., Serre, C., Gillet, B., Sebrie, C., Baati, T., & Férey, G. (2010). Porous metal-organic-framework nanoscale carriers as a potential platform for drug delivery and imaging. *Nature Materials, 9*(2), 172-178.

3. Simon-Yarza, T., Mielcarek, A., Couvreur, P., & Serre, C. (2017). Nanoparticles of metal-organic frameworks: On the road to in vivo efficacy in biomedicine. *Advanced Materials, 29*(38), 1606806.

4. Lan, G., Ni, K., & Lin, W. (2018). Nanoscale metal-organic frameworks for phototherapy of cancer. *Coordination Chemistry Reviews, 379*, 65-81

5. Chui, S. S., Lo, S. M., Charmant, J. P., Orpen, A. G., & Williams, I. D. (1999). A chemically functionalizable nanoporous material [Cu3(TMA)2(H2O)3]n. *Science, 283*(5405), 1148-1150.

6. Horcajada, P., Serre, C., Vallet-Regí, M., Sebban, M., Taulelle, F., & Férey, G. (2006). Metal-organic frameworks as efficient materials for drug delivery. *Angewandte Chemie International Edition, 45*(36), 5974-5978.

7. Cavka, J. H., Jakobsen, S., Olsbye, U., Guillou, N., Lamberti, C., Bordiga, S., & Lillerud, K. P. (2008). A new zirconium inorganic building brick forming metal organic frameworks with exceptional stability. *Journal of the American Chemical Society, 130*(42), 13850-13851.

8. Pan, Y., Liu, Y., Zeng, G., Zhao, L., & Lai, Z. (2012). Rapid synthesis of zeolitic imidazolate framework-8 (ZIF-8) nanocrystals in an aqueous system. *Chemical Communications, 48*(27), 3768-3770. https://doi.org/10.1039/c2cc30763j

9. Sharmin, E.; Zafar, F. Introductory Chapter: metal-organic frameworks (MOFs). *Metal-organic frameworks; InTech, 2016; pp 1- 16*; DOI: 10.5772/64797

10. Wiśniewska, P., Haponiuk, J., Saeb, M. R., Rabiee, N., & Bencherif, S. A. (2023). Mitigating Metal-Organic Framework (MOF) Toxicity for Biomedical Applications. *Chemical engineering journal* (Lausanne, Switzerland : 1996), 471, 144400. https://doi.org/10.1016/j.cej.2023.144400

11. Giménez-Marqués, M., Bellido, E., Berthelot, T., Simón-Yarza, T., Hidalgo, T., Simón-Vázquez, R., González-Fernández, Á., Avila, J., Asensio, M. C., Gref, R., Couvreur, P., Serre, C., & Horcajada, P. (2018). GraftFast Surface Engineering to Improve MOF Nanoparticles Furtiveness. *Small (Weinheim an der Bergstrasse, Germany)*, *14*(40), e1801900. https://doi.org/10.1002/smll.201801900

12. Agostoni, V., Horcajada, P., Noiray, M., Malanga, M., Aykaç, A., Jicsinszky, L., Vargas-Berenguel, A., Semiramoth, N., Daoud-Mahammed, S., Nicolas, V., Martineau, C., Taulelle, F., Vigneron, J., Etcheberry, A., Serre, C., & Gref, R. (2015). A "green" strategy to construct non-covalent, stable and bioactive coatings on porous MOF nanoparticles. *Scientific reports*, *5*, 7925. https://doi.org/10.1038/srep07925

13. Bellido, E., Hidalgo, T., Lozano, M. V., Guillevic, M., Simón-Vázquez, R., Santander-Ortega, M. J., González-Fernández, Á., Serre, C., Alonso, M. J., & Horcajada, P. (2015). Heparin-engineered mesoporous iron metal-organic framework nanoparticles: toward stealth drug nanocarriers. *Advanced healthcare materials*, *4*(8), 1246–1257. https://doi.org/10.1002/adhm.201400755

14. Abánades Lázaro, I., Haddad, S., Rodrigo-Muñoz, J. M., Marshall, R. J., Sastre, B., Del Pozo, V., Fairen-Jimenez, D., & Forgan, R. S. (2018). Surface-Functionalisation of Zr-Fumarate MOF for Selective Cytotoxicity and Immune System Compatibility in Nanoscale Drug Delivery. *ACS applied materials & interfaces*, *10*(37), 31146–31157. https://doi.org/10.1021/acsami.8b11652

15. Abánades Lázaro, I., Haddad, S., Sacca, S., Orellana-Tavra, C., Fairen-Jimenez, D., & Forgan, R. S. (2017). Selective Surface PEGylation of UiO-66 Nanoparticles for Enhanced Stability, Cell Uptake, and pH-Responsive Drug Delivery. *Chem*, *2*(4), 561–578. https://doi.org/10.1016/j.chempr.2017.02.005

16. Ettlinger, R., Sönksen, M., Graf, M., Moreno, N., Denysenko, D., Volkmer, D., Kerl, K., & Bunzen, H. (2018). Metal-organic framework nanoparticles for arsenic trioxide drug delivery. Journal of Materials Chemistry B, 6(39), 6481–6489. https://doi.org/10.1039/C8TB01899E

17. Ettlinger, R., Moreno, N., Volkmer, D., Kerl, K., & Bunzen, H. (2019). Zeolitic Imidazolate Framework-8 as pH-Sensitive Nanocarrier for "Arsenic Trioxide" Drug Delivery. *Chemistry (Weinheim an der Bergstrasse, Germany)*, *25*(57), 13189–13196. https://doi.org/10.1002/chem.201902599

18. Serag, E., El-Fakharany, E., Hammad, S., & El-Khouly, M. (2025). Metal–organic framework MIL-101(Fe) functionalized with folic acid as a multifunctional nanocarrier for targeted chemotherapy–photodynamic therapy. *Biomaterials Science, 13,* — Article in Press. https://doi.org/10.1039/d4bm01738b

19. Wu, H., Liu, Y., Chen, L., Wang, S., Liu, C., Zhao, H., Jin, M., Chang, S., Quan, X., Cui, M., Wan, H., Gao, Z., & Huang, W. (2022). Combined Biomimetic MOF-RVG15 Nanoformulation Efficient Over BBB for Effective Anti-Glioblastoma in Mice Model. *International journal of nanomedicine*, *17*, 6377–6398. https://doi.org/10.2147/IJN.S387715

20. Cedervall, T., Lynch, I., Lindman, S., Berggård, T., Thulin, E., Nilsson, H., Dawson, K. A., & Linse, S. (2007). Understanding the nanoparticle-protein corona using methods to quantify exchange rates and affinities of proteins for nanoparticles. *Proceedings of the National Academy of Sciences of the United States of America, 104*(7), 2050-2055. https://doi.org/10.1073/pnas.0608582104

21. González-García, L. E., MacGregor, M. N., Visalakshan, R. M., Lazarian, A., Cavallaro, A. A., Morsbach, S., Mierczynska-Vasilev, A., Mailänder, V., Landfester, K., & Vasilev, K. (2022). Nanoparticles Surface Chemistry Influence on Protein Corona Composition and Inflammatory Responses. *Nanomaterials*, *12*(4), 682. https://doi.org/10.3390/nano12040682

22. Ruenraroengsak, P., Novak, P., Berhanu, D., Thorley, A. J., Valsami-Jones, E., Gorelik, J., Korchev, Y. E., & Tetley, T. D. (2012). Respiratory epithelial cytotoxicity and membrane damage (holes) caused by amine-modified nanoparticles. *Nanotoxicology*, *6*(1), 94-108. https://doi.org/10.3109/17435390.2011.558643

23. Li, S., Dharmarwardana, M., Welch, R. P., Benjamin, C. E., Shamir, A. M., Nielsen, S. O., & Gassensmith, J. J. (2018). Investigation of controlled growth of metal-organic frameworks on anisotropic virus particles. *Journal of the American Chemical Society, 140*(46), 15132-15141. https://doi.org/10.1021/jacs.8b04457

24. Wuttke, S., Zimpel, A., Bein, T., Braig, S., Stoiber, K., Vollmar, A. (2017). MOF nanoparticles in biomedical applications. *Chemical Reviews, 117*(2), 1237-1318.

25. Jafari, S., Izadi, Z., Alaei, L., Yazdian, F., & Omidi, M. (2020). Human plasma protein corona decreases the toxicity of pillar-layer metal–organic framework. *Scientific Reports, 10,* 14569. https://doi.org/10.1038/s41598-020-71170-z

26. Gao, M., Yang, C., Wu, C., Chen, Y., Zhuang, H., Wang, J., & Cao, Z. (2022). Hydrogel-metal-organic-framework hybrids mediated efficient oral delivery of siRNA for the treatment of ulcerative colitis. *Journal of nanobiotechnology*, *20*(1), 404. https://doi.org/10.1186/s12951-022-01603-6

27. Chen, Q., Wang, J., Xiong, X., Chen, J., Wang, B., Yang, H., Zhou, J., Deng, H., Gu, L., & Tian, J. (2024). Blood-Brain Barrier-Penetrating Metal-Organic Framework Antioxidant Nanozymes for Targeted Ischemic Stroke Therapy. *Advanced healthcare materials*, e2402376. Advance online publication. https://doi.org/10.1002/adhm.202402376

28. Baati, T., Njim, L., Neffati, F., Kerkeni, A., Bouttemi, M., Gref, R., … Horcajada, P. (2020). In depth analysis of the in vivo biocompatibility of porous iron(III) metal-organic frameworks. *Advanced Materials, 32*(5), 1907276. https://doi.org/10.1002/adma.201907276

29. Wang, Y., Zhou, J., & Li, J. (2012). Lysosome: A new hub for nanomaterial toxicity. *Cell Death & Disease, 3*, e403. https://doi.org/10.1038/cddis.2012.139

30. Ettlinger, R., Lächelt, U., Gref, R., Horcajada, P., Lammers, T., Serre, C., Couvreur, P., Morris, R. E., & Wuttke, S. (2023). Correction: Toxicity of metal-organic framework nanoparticles: from essential analyses to potential applications. *Chemical Society reviews, 52*(3), 1156. https://doi.org/10.1039/d3cs90014b

31. Wuttke, S., Braig, S., Preiß, T., Zimpel, A., Sicklinger, J., Bellomo, C., … Bein, T. (2015). MOF nanoparticles: Toxicity and cellular uptake. *Chemical Communications, 51*(83), 15752-15755. https://doi.org/10.1039/C5CC06172J

32. Lin, J., Huang, L., Ou, H., Chen, A., Xiang, R., & Liu, Z. (2021). Effects of ZIF-8 MOFs on structure and function of blood components. *RSC advances*, *11*(35), 21414–21425. https://doi.org/10.1039/d1ra02873a

33. Duan, W., Qiao, S., Zhuo, M., Sun, J., Guo, M., Xu, F., Liu, J., Wang, T., Guo, X., Zhang, Y., Gao, J., Huang, Y., Zhang, Z., Cheng, P., Ma, S., & Chen, Y. (2021). Multifunctional platforms: Metal-organic frameworks for cutaneous and cosmetic treatment. *Chem, 7*(2), 450-462. https://doi.org/10.1016/j.chempr.2020.11.018

34. Ruyra, À., Yazdi, A., Espín, J., Carné-Sánchez, A., Roher, N., Lorenzo, J., Imaz, I., & Maspoch, D. (2015). Synthesis, culture medium stability, and in vitro and in vivo zebrafish embryo toxicity of metal-organic framework nanoparticles. *Chemistry (Weinheim an der Bergstrasse, Germany)*, *21*(6), 2508-2518. https://doi.org/10.1002/chem.201405380

35. Sforna, G., Tarantino, P., Carletti, R., et al. (2020). Magnesium in biology, medicine, and nutrition. *Nutrients, 12*(11), 3438. https://doi.org/10.3390/nu12113438

36. Outten, C. E., & O'Halloran, T. V. (2001). Femtomolar sensitivity of metalloregulatory proteins controlling zinc homeostasis. *Science, 292*(5526), 2488-2492. https://doi.org/10.1126/science.1060331

37. Kawanishi, S., Inoue, S., & Sano, S. (2001). Mechanism of nickel(II)-mediated DNA damage. *Free Radical Research, 34*(5), 529-533. https://doi.org/10.1080/10715760100300471

38. Zoroddu, M. A., Aaseth, J., Crisponi, G., Medici, S., Peana, M., & Nurchi, V. M. (2019). The essential metals for humans: A brief overview. *Journal of Inorganic Biochemistry, 195*, 120-129. https://doi.org/10.1016/j.jinorgbio.2019.03.013

39. Martinez-Finley, E. J., Gavin, C. E., Aschner, M., & Gunter, T. E. (2013). Manganese neurotoxicity and the role of reactive oxygen species. *Free Radical Biology and Medicine, 62*, 65-75. https://doi.org/10.1016/j.freeradbiomed.2013.01.032

40. Gaetke, L. M., & Chow, C. K. (2003). Copper toxicity, oxidative stress, and antioxidant nutrients. *Toxicology, 189*(1-2), 147-163. https://doi.org/10.1016/S0300-483X(03)00159-8

41. Macomber, L., & Imlay, J. A. (2009). The iron-sulfur clusters of dehydratases are primary intracellular targets of copper toxicity. *Proceedings of the National Academy of Sciences, 106*(20), 8344-8349. https://doi.org/10.1073/pnas.0812808106

42. Tamames-Tabar, C., Cunha, D., Imbuluzqueta, E., Ragon, F., Serre, C., Blanco-Prieto, M. J., & Horcajada, P. (2013). Cytotoxicity of nanoscaled metal-organic frameworks. Journal of Materials Chemistry B, 2(3), 262-271. https://doi.org/10.1039/c3tb20832j

43. Ragon, F., Campo, B., Yang, Q., Martineau, C., Wiersum, A. D., Lago, A., … Serre, C. (2014). Acidic MOFs: Analysis of the stability of UiO-66 under acidic conditions. *Chemical Communications, 51*(1), 247-249. https://doi.org/10.1039/C4CC04458D

44. Yang, L., Chen, H., Kaziem, A. E., Miao, X., Huang, S., Cheng, D., Xu, H., & Zhang, Z. (2024). Effects of Exposure to Different Types of Metal-Organic Framework Nanoparticles on the Gut Microbiota and Liver Metabolism of Adult Zebrafish. *ACS nano*, *18*(37), 25425-25445. https://doi.org/10.1021/acsnano.4c03451

45. Zhang, Y., Xue, Z., Yang, Z., Chen, M., Zhou, L., Zhou, L., Zhu, M., Huang, Z., Li, Y., Kang, S., Zheng, L., & Zhang, D. (2025). Pulmonary Injury Induced via Metal-Organic Frameworks (MOFs): ROS Generation and Inflammatory Responses Mediated by HKUST-1. ACS omega, 10(17), 17865-17874. https://doi.org/10.1021/acsomega.5c00670

46. Sifaoui, I., Pacheco-Fernández, I., Piñero, J. E., Pino, V., & Lorenzo-Morales, J. (2021). A Simple *in vivo* Assay Using Amphipods for the Evaluation of Potential Biocompatible Metal-Organic

Frameworks. *Frontiers in bioengineering and biotechnology*, *9*, 584115. https://doi.org/10.3389/fbioe.2021.584115

47. Grall, R., Hidalgo, T., Delic, J., Garcia-Marquez, A., Chevillard, S., & Horcajada, P. (2015). In vitro biocompatibility of mesoporous metal (III; Fe, Al, Cr) trimesate MOF nanocarriers. *Journal of Materials Chemistry B, 3*(42), 8279-8292.

48. Singh, N., Qutub, S., & Khashab, N. M. (2021). Biocompatibility and biodegradability of metal organic frameworks for biomedical applications. *Journal of Materials Chemistry B, 9*(30), 5925-5934. https://doi.org/10.1039/d1tb01044a

49. Liu, Z., Deng, H., Zheng, Y., Tian, Y., Zhang, Y., Garcia, R. M., Garcia, S. a. H., & Yeung, K. L. (2025). Synthesis, characterization, and toxicity evaluation of Size-Dependent Iron-Based Metal-Organic frameworks. Nanomaterials, 15(12), 927. https://doi.org/10.3390/nano15120927

50. Horcajada, P., Chalati, T., Serre, C., Gillet, B., Sebrie, C., Baati, T., Eubank, J. F., Heurtaux, D., Clayette, P., Kreuz, C., Chang, J. S., Hwang, Y. K., Marsaud, V., Bories, P. N., Cynober, L., Gil, S., Férey, G., Couvreur, P., & Gref, R. (2010). Porous metal-organic-framework nanoscale carriers as a potential platform for drug delivery and imaging. *Nature materials*, *9*(2), 172-178. https://doi.org/10.1038/nmat2608

51. Chui, S. S.-Y., Lo, S. M.-F., Charmant, J. P. H., Orpen, A. G., & Williams, I. D. (1999). A chemically functionalizable nanoporous material $[Cu_3(TMA)_2(H_2O)_3]$□. *Science, 283*(5405), 1148-1150. https://doi.org/10.1126/science.283.5405.1148

52. Férey, G., Mellot-Draznieks, C., Serre, C., Millange, F., Dutour, J., Surblé, S., & Margiolaki, I. (2005). A chromium terephthalate-based solid with unusually large pore volumes and surface area. *Science, 309*(5743), 2040-2042. https://doi.org/10.1126/science.1116275

53. Behzadi, S., Serpooshan, V., Tao, W., Hamaly, M. A., Alkawareek, M. Y., Dreaden, E. C., … Mahmoudi, M. (2017). Cellular uptake of nanoparticles: Journey inside the cell. *Chemical Society Reviews, 46*(14), 4218-4244. https://doi.org/10.1039/C6CS00636A

54. Albanese, A., Tang, P. S., & Chan, W. C. W. (2012). The effect of nanoparticle size, shape, and surface chemistry on biological systems. *Annual Review of Biomedical Engineering, 14*(1), 1-16. https://doi.org/10.1146/annurev-bioeng-071811-150124

55. Blanco, E., Shen, H., & Ferrari, M. (2015). Principles of nanoparticle design for overcoming biological barriers to drug delivery. *Nature Biotechnology, 33*(9), 941-951. https://doi.org/10.1038/nbt.3330

56. Chen, P., He, M., Chen, B., & Hu, B. (2020). Size- and dose-dependent cytotoxicity of ZIF-8 based on single cell analysis. *Ecotoxicology and environmental safety*, *205*, 111110. https://doi.org/10.1016/j.ecoenv.2020.111110

57. Hao, F., Yan, Z. Y., & Yan, X. P. (2022). Recent Advances in Research on the Effect of Physicochemical Properties on the Cytotoxicity of Metal-Organic Frameworks. *Small science*, *2*(9), 2200044. https://doi.org/10.1002/smsc.202200044

58. Zhu, Z., Jiang, S., Liu, Y. et al. (2020). Micro or nano: Evaluation of biosafety and biopotency of magnesium metal organic framework-74 with different particle sizes. Nano Res. 13, 511-526. https://doi.org/10.1007/s12274-020-2642-y

59. Jiang, S., Wang, J., Zhu, Z., Shan, S., Mao, Y., Zhang, X., Pei, X., Huang, C., & Wan, Q. (2022). The synthesis of nano bio-MOF-1 with a systematic evaluation on the biosafety and biocompatibility. *Microporous and Mesoporous Materials, 334,* 111773. https://doi.org/10.1016/j.micromeso.2022.111773

60. Cambridge Crystallographic Data Centre. (n.d.). *CSD MOF collection.* Cambridge Crystallographic Data Centre. Retrieved September 12, 2025, from https://www.ccdc.cam.ac.uk/free-products/csd-mof-collection/

Tables and Figures

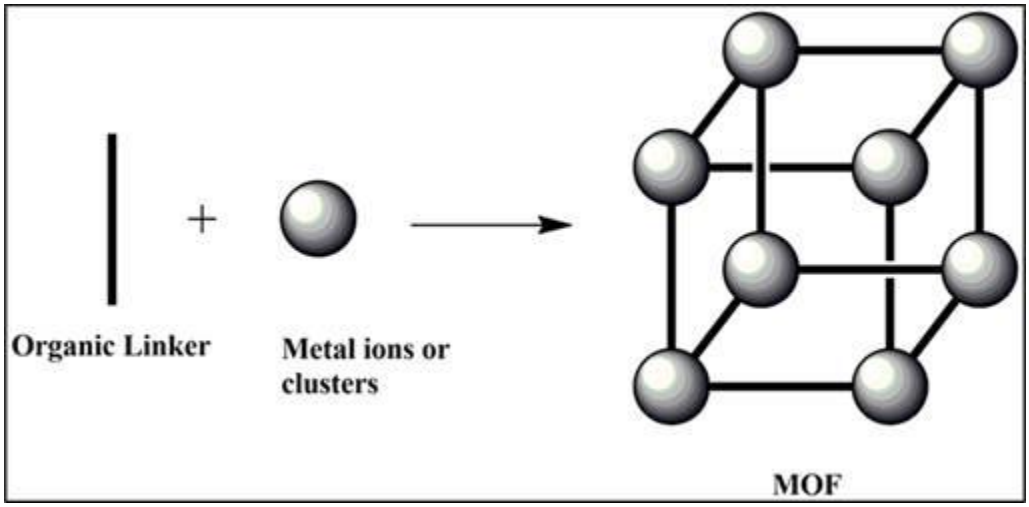

Figure 1: Structure of MOF (Sharmin & Zafar, 2016; pp4)[9]

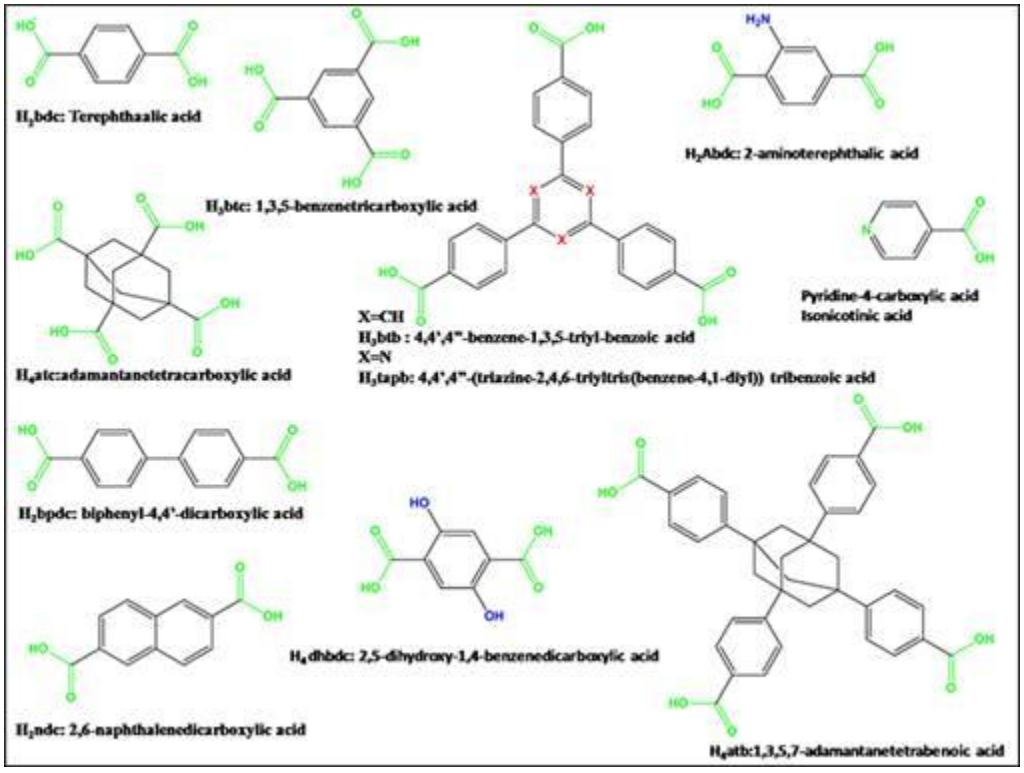

Figure 2: Examples of organic ligands with carboxylic functionality used in MOFs (Sharmin & Zafar, 2016; pp6)[9]

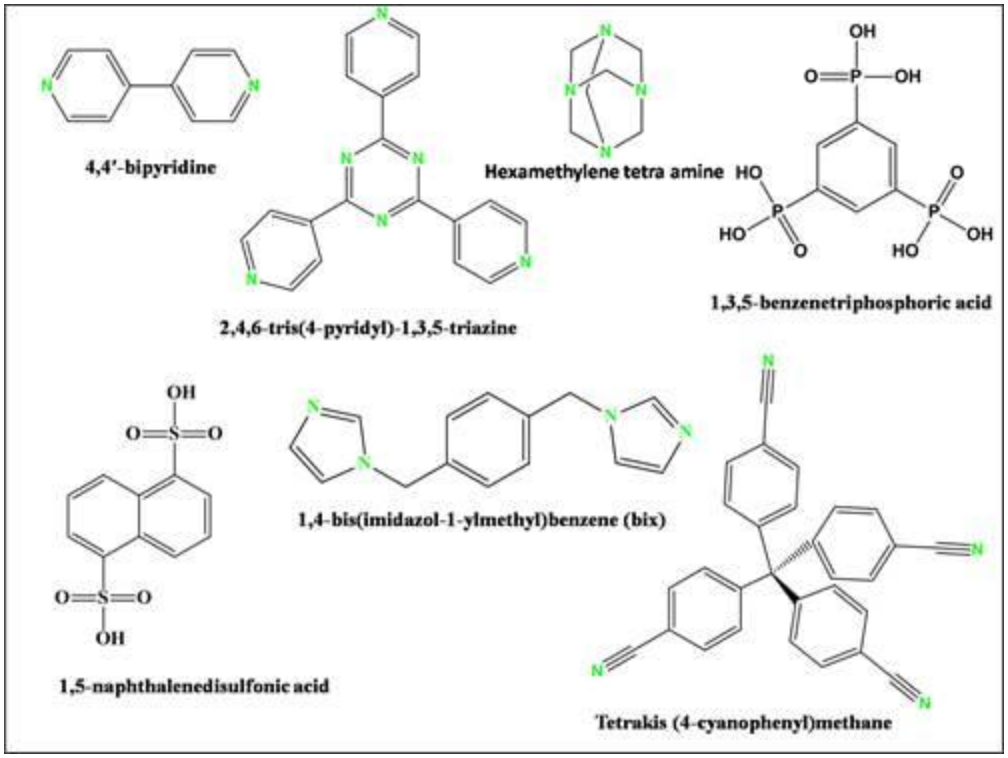

Figure 3: Examples of ligands containing nitrogen, sulphur, phosphorous and heterocycles used in MOFs (Sharmin & Zafar, 2016; pp7)[9]

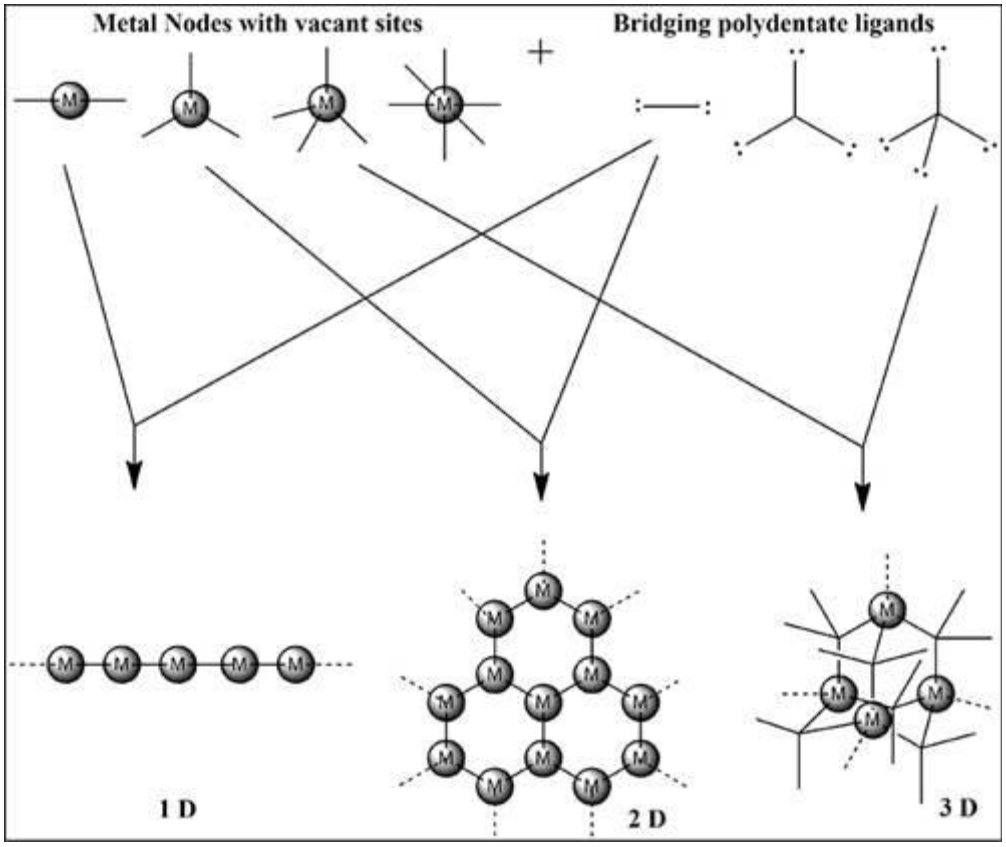

Figure 4: MOFs resulting from different metal nodes and bridging ligands (Sharmin & Zafar, 2016; pp7)[9]

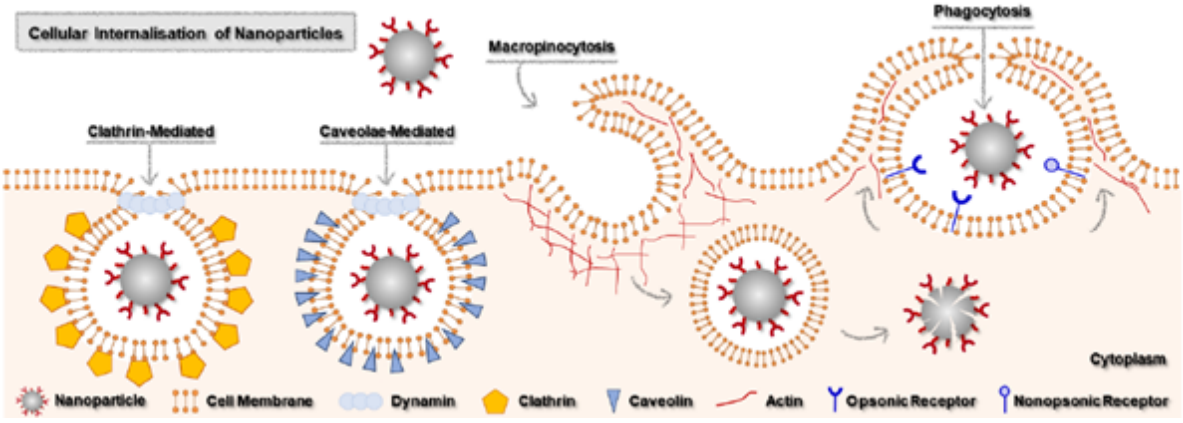

Figure 5: Different mechanisms of cellular internalizations of nanoparticles (Ettlinger et al., 2023; pp4)[30]

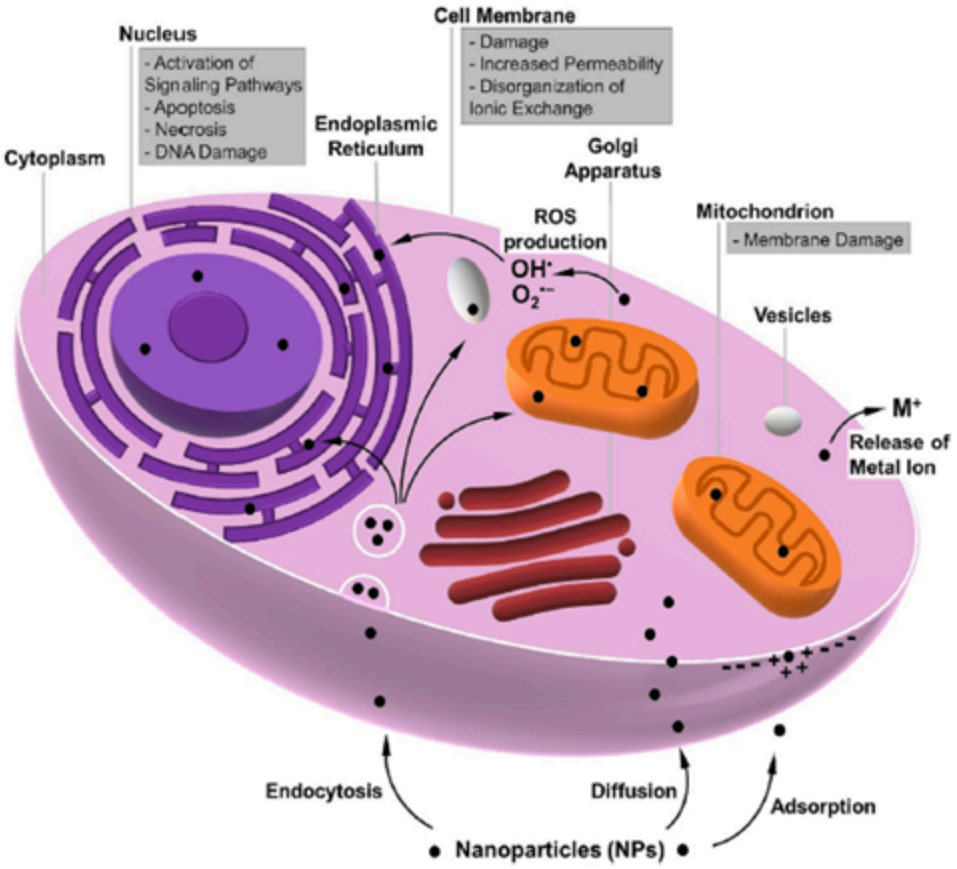

Figure 6: Schematic illustration of the main mechanisms associated with MOF-induced toxicity (Wiśniewska et al., 2023; pp6)[10]

#	MOF	Metal node	Linker	Function-alization	Size (nm)	Cell line / Model	Type	Exposure	IC_{50}/ LC_{50}/ Cell viability %	Measure	Source
1	Mg-MOF-74	Mg	H4DHTP	-	-	HepG2	In-vitro	200 µM; 72h	96	Cell viability (%)	Ruyra A., et al. (2015)
	Co-MOF-74	Co	H4DHTP	-	-	HepG2	In-vitro	200 µM; 72h	75	Cell viability (%)	Ruyra A., et al. (2015)
	Ni-MOF-74	Ni	H4DHTP	-	-	HepG2	In-vitro	200 µM; 72h	68	Cell viability (%)	Ruyra A., et al. (2015)
	Zn-MOF-74	Zn	H4DHTP	-	-	HepG2	In-vitro	200 µM; 72h	68	Cell viability (%)	Ruyra A., et al. (2015)
	Mn-MOF-74	Mn	H4DHTP	-	-	HepG2	In-vitro	200 µM; 72h	18	Cell viability (%)	Ruyra A., et al. (2015)
	Cu-MOF-74	Cu	H4DHTP	-	-	HepG2	In-vitro	200 µM; 72h	0	Cell viability (%)	Ruyra A., et al. (2015)
2	MIL-88B	Fe	H2BDC	(H)1–4	100	J774	In-vitro	24h	370	IC_{50} (µg/mL)	Tamames-Tabar, C. et al. (2013)
	UiO-66	Zr	H2BDC	(H)1–4	100	J774	In-vitro	24h	60	IC_{50} (µg/mL)	Tamames-Tabar, C. et al. (2013)
	MIL-88B	Fe	H2BDC	(H)1–4	100	HeLa	In-vitro	24h	1260	IC_{50} (µg/mL)	Tamames-Tabar, C. et al. (2013)
	UiO-66	Zr	H2BDC	(H)1–4	100	HeLa	In-vitro	24h	400	IC_{50} (µg/mL)	Tamames-Tabar, C. et al. (2013)
3	MIL-101(Fe)-NH_2	Fe	H2BDC	NH_2	-	Zebrafish	In-vivo	96h	>400	LC_{50} (µg/mL)	Yang et al. (2024)
	UiO-66-NH_2	Zr	H2BDC	NH_2	-	Zebrafish	In-vivo	96h	>400	LC_{50} (µg/mL)	Yang et al. (2024)
	ZIF-8	Zn	MIM	-	-	Zebrafish	In-vivo	96h	143.47	LC_{50} (µg/mL)	Yang et al. (2024)
	ZIF-90	Zn	HICA	-	-	Zebrafish	In-vivo	96h	19.61	LC_{50} (µg/mL)	Yang et al. (2024)
	HKUST-1	Cu	BTC3-	-	-	Zebrafish	In-vivo	96h	1.97	LC_{50} (µg/mL)	Yang et al. (2024)
4	UiO-66	Zr	H2BDC	(H)1–4	30-100	BEAS-2B	In-vitro	200 µg/ml; 24h	90	Cell viability (%)	Zhang Y., et al (2025)
	HKUST-1	Cu	BTC3-	-	30-100	BEAS-2B	In-vitro	200 µg/ml; 24h	10	Cell viability (%)	Zhang Y., et al (2025)
5	CIM-80	Al	2-methyl-2-butenedioic acid	-	-	J774	In-vitro	24h	>5000	LC_{50} (µg/mL)	Sifaoui I., et al. (2021)
	CIM-84	Zr	2-methyl-2-butenedioic acid	-	-	J774	In-vitro	24h	>5000	LC_{50} (µg/mL)	Sifaoui I., et al. (2021)
	UiO-66	Zr	H2BDC	-	-	J774	In-vitro	24h	>5000	LC_{50} (µg/mL)	Sifaoui I., et al. (2021)
	CIM-81	Zn	1,2,4-triazole +H2BDC	-	-	J774	In-vitro	24h	980	LC_{50} (µg/mL)	Sifaoui I., et al. (2021)
	CIM-91	Zn	1,2,4-triazole +H2BDC	-	-	J774	In-vitro	24h	880	LC_{50} (µg/mL)	Sifaoui I., et al. (2021)
6	MIL-100 (Fe)	Fe	H3BTC	-	252	A549	In-vitro	64 µg/cm^2; 24h	95	Cell viability (%)	Grall et al. (2015)
	MIL-100 (Al)	Al	H3BTC	-	311	A549	In-vitro	64 µg/cm^2; 24h	97	Cell viability (%)	Grall et al. (2015)
	MIL-100 (Cr)	Cr	H3BTC	-	146	A549	In-vitro	64 µg/cm^2; 24h	99	Cell viability (%)	Grall et al. (2015)
	MIL-100 (Fe)	Fe	H3BTC	-	252	Hep3B	In-vitro	64 µg/cm^2; 24h	60	Cell viability (%)	Grall et al. (2015)
	MIL-100 (Al)	Al	H3BTC	-	311	Hep3B	In-vitro	64 µg/cm^2; 24h	80	Cell viability (%)	Grall et al. (2015)
	MIL-100 (Cr)	Cr	H3BTC	-	146	Hep3B	In-vitro	64 µg/cm^2; 24h	82	Cell viability (%)	Grall et al. (2015)

H2BDC: 1,4-benzenedicarboxylic acid, also known as terephthalic acid
BDC2-: 1,4-benzenedicarboxylate, the deprotonated form of terephthalic acid (H2BDC)
BTC3-: 1,3,5-benzenetricarboxylate, which is the deprotonated form of 1,3,5-benzenetricarboxylic acid, also known as trimesic acid.
MIM: 2-methylimidazolate.
HICA: 1H-imidazole-2-carbaldehyde
H3BTC: 1,3,5-benzenetricarboxylic acid, also known as trimesic acid
H4DHTP: 2,5-Dihydroxyterephthalic acid

Figure 7: MOF cytotoxicity with metal node as key variable parameter

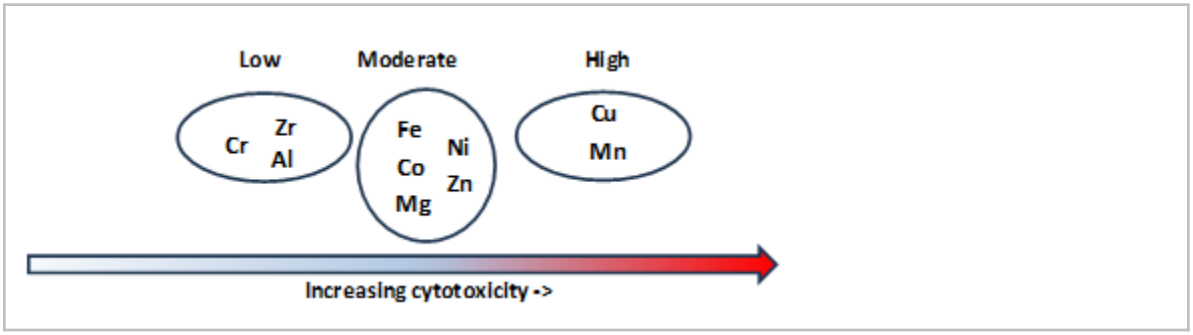

Figure 8: Assessed cytotoxicity trend comparing different metal nodes

#	MOF	Metal node	Linker	Size (nm)	Cell line / Model	Type	Exposure	MOF cytotoxicity value	Linker cytotoxicity value	MOF/Linker cytotoxicity measure	Source
1	MIL-100(Fe)	Fe	H3BTC	120	J774	In-vitro	24h	700	>1000	IC_{50} (µg/mL)	Tamames-Tabar, C. et al (2013)
	MIL-127	Fe	Tazb	476	J774	In-vitro	24h	440	820	IC_{50} (µg/mL)	Tamames-Tabar, C. et al (2013)
	MIL-88B	Fe	H2BDC	100	J774	In-vitro	24h	370	430	IC_{50} (µg/mL)	Tamames-Tabar, C. et al (2013)
	MIL-88A	Fe	FUM	105	J774	In-vitro	24h	50	400	IC_{50} (µg/mL)	Tamames-Tabar, C. et al (2013)
2	MIL-100(Fe)	Fe	H3BTC	120	HeLa	In-vitro	24h	1100	2000	IC_{50} (µg/mL)	Tamames-Tabar, C. et al (2013)
	MIL-127	Fe	Tazb	476	HeLa	In-vitro	24h	>2000	800	IC_{50} (µg/mL)	Tamames-Tabar, C. et al (2013)
	MIL-88B	Fe	H2BDC	100	HeLa	In-vitro	24h	1260	800	IC_{50} (µg/mL)	Tamames-Tabar, C. et al (2013)
	MIL-88A	Fe	FUM	105	HeLa	In-vitro	24h	15	30	IC_{50} (µg/mL)	Tamames-Tabar, C. et al (2013)
3	MIL-101(Fe)	Fe	H2BDC	968	A549	In-vitro	100 µg/ml; 24h	58		Cell viability (%)	Liu, Z., et al (2025)
	MIL-88A	Fe	FUM	1128	A549	In-vitro	100 µg/ml; 24h	10		Cell viability (%)	Liu, Z., et al (2025)
4	NOTT-100	Cu	BPTC	50	HepG2	In-vitro	200 µM; 72h	5	85	Cell viability (%)	Ruyra A., et al. (2015)
	HKUST-1	Cu	H3BTC	60	HepG2	In-vitro	200 µM; 72h	0	79	Cell viability (%)	Ruyra A., et al. (2015)
	UiO-66	Zr	H2BDC	30	HepG2	In-vitro	200 µM; 72h	96	85	Cell viability (%)	Ruyra A., et al. (2015)
	UiO-67	Zr	BPDC	150	HepG2	In-vitro	200 µM; 72h	98	95	Cell viability (%)	Ruyra A., et al. (2015)
	MIL-100(Fe)	Fe	H3BTC	100	HepG2	In-vitro	200 µM; 72h	80	79	Cell viability (%)	Ruyra A., et al. (2015)
	MIL-101(Fe)	Fe	H2BDC	110	HepG2	In-vitro	200 µM; 72h	45	81	Cell viability (%)	Ruyra A., et al. (2015)
	ZIF-7	Zn	BIM	300	HepG2	In-vitro	200 µM; 72h	85	78	Cell viability (%)	Ruyra A., et al. (2015)
	ZIF-8	Zn	MIM	110	HepG2	In-vitro	200 µM; 72h	40	85	Cell viability (%)	Ruyra A., et al. (2015)
5	ZIF-8	Zn	MIM	-	Zebrafish	In-vivo	96h	143.47		LC_{50} (µg/mL)	Yang et al. (2024)
	ZIF-90	Zn	HICA	-	Zebrafish	In-vivo	96h	19.61		LC_{50} (µg/mL)	Yang et al. (2024)

H2BDC: 1,4-benzenedicarboxylic acid, also known as terephthalic acid
H3BTC: 1,3,5-benzenetricarboxylic acid, also known as trimesic acid
BPTC: biphenyl-3,3',5,5'-tetracarboxylate
Tabz: azobenzenetetracarboxylic acid
FUM: fumaric acid (trans-(E) isomer of 2-butenedioic acid)
MIM: 2-methylimidazolate.
HICA: 1H-imidazole-2-carbaldehyde
BPDC: 4,4'-biphenyldicarboxylic acid
BIM: benzimidazole

Figure 9: MOF/Linker cytotoxicity with organic linker as key variable parameter

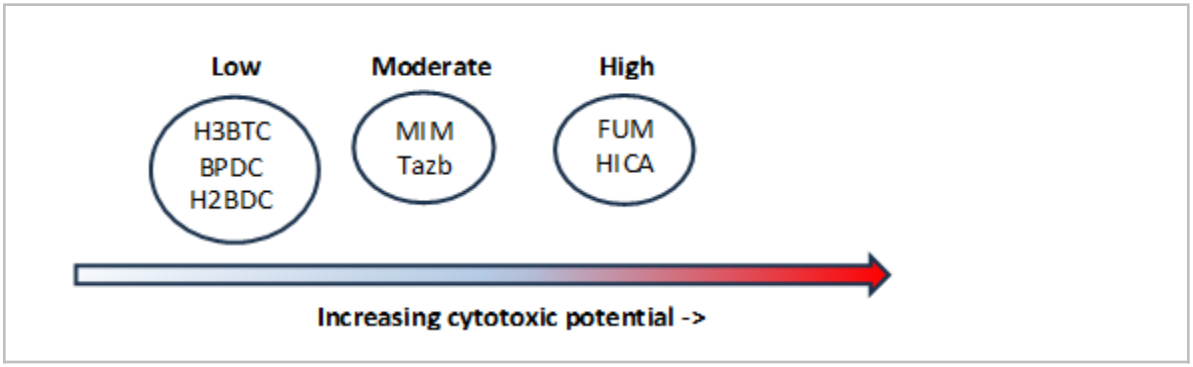

Figure 10: Linker relative cytotoxic potential

#	MOF	Metal node	Linker	Functionalization	Polarity	Size (nm)	Cell line / Model	Type	Exposure	MOF cytotoxicity value	MOF cytotoxicity measure	Source
1	MIL-101(Fe)_2CH3	Fe	H2BDC	(CH3)1,3(H)2,4	Non-polar	120	HeLa	In-vitro	24h	>2500	IC_{50} (µg/mL)	Tamames-Tabar, C. et al (2013)
	MIL-101_NH2	Fe	H2BDC	(NH2)1,(H)2–4	Polar	100	HeLa	In-vitro	24h	>1000	IC_{50} (µg/mL)	Tamames-Tabar, C. et al (2013)
	MIL-101(Fe)_2CH3	Fe	H2BDC	(CH3)1,3(H)2,4	Non-polar	120	J774	In-vitro	24h	170	IC_{50} (µg/mL)	Tamames-Tabar, C. et al (2013)
	MIL-101_NH2	Fe	H2BDC	(NH2)1,(H)2–4	Polar	100	J774	In-vitro	24h	70	IC_{50} (µg/mL)	Tamames-Tabar, C. et al (2013)
2	MIL-88B	Fe	H2BDC	(H)1–4	Polar	100	HeLa	In-vitro	24h	1260	IC_{50} (µg/mL)	Tamames-Tabar, C. et al (2013)
	MIL-88B_NH2	Fe	H2BDC	(NH2)1,(H)2–4	Polar	115	HeLa	In-vitro	24h	1100	IC_{50} (µg/mL)	Tamames-Tabar, C. et al (2013)
	MIL-88B_NO2	Fe	H2BDC	(NO2)1,(H)2–4	Polar	130	HeLa	In-vitro	24h	>2000	IC_{50} (µg/mL)	Tamames-Tabar, C. et al (2013)
	MIL-88B_CH3	Fe	H2BDC	(CH3)1,(H)2–4	Non-polar	75	HeLa	In-vitro	24h	>2000	IC_{50} (µg/mL)	Tamames-Tabar, C. et al (2013)
	MIL-88B_2CH3	Fe	H2BDC	(CH3)1,3(H)2,4	Non-polar	100	HeLa	In-vitro	24h	2100	IC_{50} (µg/mL)	Tamames-Tabar, C. et al (2013)
	MIL-88B_4CH3	Fe	H2BDC	(CH3)1–4	Non-polar	120	HeLa	In-vitro	24h	690	IC_{50} (µg/mL)	Tamames-Tabar, C. et al (2013)
	MIL-88B_2CF3	Fe	H2BDC	(CF3)1,3(H)2,4	Non-polar	105	HeLa	In-vitro	24h	>2000	IC_{50} (µg/mL)	Tamames-Tabar, C. et al (2013)
	MIL-88B	Fe	H2BDC	(H)1–4	Polar	100	J774	In-vitro	24h	370	IC_{50} (µg/mL)	Tamames-Tabar, C. et al (2013)
	MIL-88B_NH2	Fe	H2BDC	(NH2)1,(H)2–4	Polar	115	J774	In-vitro	24h	450	IC_{50} (µg/mL)	Tamames-Tabar, C. et al (2013)
	MIL-88B_NO2	Fe	H2BDC	(NO2)1,(H)2–4	Polar	130	J774	In-vitro	24h	30	IC_{50} (µg/mL)	Tamames-Tabar, C. et al (2013)
	MIL-88B_CH3	Fe	H2BDC	(CH3)1,(H)2–4	Non-polar	75	J774	In-vitro	24h	370	IC_{50} (µg/mL)	Tamames-Tabar, C. et al (2013)
	MIL-88B_2CH3	Fe	H2BDC	(CH3)1,3(H)2,4	Non-polar	100	J774	In-vitro	24h	360	IC_{50} (µg/mL)	Tamames-Tabar, C. et al (2013)
	MIL-88B_4CH3	Fe	H2BDC	(CH3)1–4	Non-polar	120	J774	In-vitro	24h	80	IC_{50} (µg/mL)	Tamames-Tabar, C. et al (2013)
	MIL-88B_2CF3	Fe	H2BDC	(CF3)1,3(H)2,4	Non-polar	105	J774	In-vitro	24h	410	IC_{50} (µg/mL)	Tamames-Tabar, C. et al (2013)
3	UiO-66	Zr	H2BDC	-	-	30	HepG2	In-vitro	200 µM; 72h	96	Cell viability (%)	Ruyra A., et al. (2015)
	UiO-66-NH_2	Zr	H2BDC	NH2	Polar	70	HepG2	In-vitro	200 µM; 72h	75	Cell viability (%)	Ruyra A., et al. (2015)

H2BDC: 1,4-benzenedicarboxylic acid, also known as terephthalic acid

Figure 11: MOF functionalisation and cytotoxicity

#	MOF	Metal node	Linker	Size (nm)	Cell line / Model	Type	Exposure	MOF cytotoxicity value	MOF cytotoxicity measure	Source
1	MIL-101(Fe)	Fe	H2BDC	236	A549	In-vitro	100 µg/ml; 24h	42	Cell viability (%)	Liu, Z., et al (2025)
	MIL-101(Fe)	Fe	H2BDC	487	A549	In-vitro	100 µg/ml; 24h	52	Cell viability (%)	Liu, Z., et al (2025)
	MIL-101(Fe)	Fe	H2BDC	968	A549	In-vitro	100 µg/ml; 24h	54	Cell viability (%)	Liu, Z., et al (2025)
	MIL-88A	Fe	FUM	1128	A549	In-vitro	100 µg/ml; 24h	9	Cell viability (%)	Liu, Z., et al (2025)
	MIL-88A	Fe	FUM	3474	A549	In-vitro	100 µg/ml; 24h	22	Cell viability (%)	Liu, Z., et al (2025)
	MIL-88A	Fe	FUM	4894	A549	In-vitro	100 µg/ml; 24h	45	Cell viability (%)	Liu, Z., et al (2025)
2	ZIF-8	Zn	2-methylimidazolate	50	HepG2	In-vitro	24h	15.6	IC_{50} (µg/mL)	Chen et al. (2020)
	ZIF-8	Zn	2-methylimidazolate	90	HepG2	In-vitro	24h	17.5	IC_{50} (µg/mL)	Chen et al. (2020)
	ZIF-8	Zn	2-methylimidazolate	200	HepG2	In-vitro	24h	19.7	IC_{50} (µg/mL)	Chen et al. (2020)
3	PCN-224	Zr	TCPP	30	J774	In-vitro	24h	35	IC_{50} (nM)	Hao F., et al. (2022)
	PCN-224	Zr	TCPP	90	J774	In-vitro	24h	50	IC_{50} (nM)	Hao F., et al. (2022)
	PCN-224	Zr	TCPP	180	J774	In-vitro	24h	100	IC_{50} (nM)	Hao F., et al. (2022)
4	nMg-MOF-74	Mg	H4DHTP	300	J774	In-vitro	24h	>2000	IC_{50} (µg/mL)	Zhu Z et al., (2020)
	mMg-MOF-74	Mg	H4DHTP	3700	J774	In-vitro	24h	798	IC_{50} (µg/mL)	Zhu Z et al., (2020)
5	nBio-MOF-1	Zn	BPDC+adenine	594	MC3T3-E1	In-vitro	24h	599	IC_{50} (µg/mL)	Jiang et al. (2022)
	mBio-MOF-1	Zn	BPDC+adenine	65842	MC3T3-E1	In-vitro	24h	248	IC_{50} (µg/mL)	Jiang et al. (2022)

H2BDC: 1,4-benzenedicarboxylic acid, also known as terephthalic acid
FUM: fumaric acid (trans-(E) isomer of 2-butenedioic acid)
TCPP: 5,10,15,20-tetrakis(4-carboxyphenyl)porphyrin
H4DHTP: 2,5-Dihydroxyterephthalic acid
BPDC: biphenyldicarboxylate

Figure 12: MOF particle size and cytotoxicity